antioxidants

MDPI

Article

Effect of *Hericium erinaceus* May Be Polysaccharide-Rich Extract on Production Performance, Immune Organ Histology, Immune and Antioxidant Status, and Cellular Proliferation and Apoptosis in Heat-Stressed Broilers

Chaohui Zhang [1], Yuxuan Zheng [1], Jinjing Wang [1], Chenfang Wang [1], Man Ren [1], Weiwei Wang [1], Chunfang Zhao [1], Jian Tu [2], Wei Chen [3], Shenghe Li [1] and Erhui Jin [1,4,*]

[1] College of Animal Science, Anhui Science and Technology University, Chuzhou 233100, China; zhangchaohui@ahstu.edu.cn (C.Z.); zhengyuxuan@ahstu.edu.cn (Y.Z.); wangjinjing@ahstu.edu.cn (J.W.); wangcf@ahstu.edu.cn (C.W.); renman@ahstu.edu.cn (M.R.); weiweiwang@ahstu.edu.cn (W.W.); zhaocf@ahstu.edu.cn (C.Z.); lish@ahstu.edu.cn (S.L.)
[2] College of Veterinary Medicine, Anhui Agricultural University, Hefei 230036, China; tujian1980@ahau.edu.cn
[3] State Key Laboratory of Swine and Poultry Breeding Industry, Institute of Animal Science, Guangdong Academy of Agricultural Sciences, State Key Laboratory of Livestock and Poultry Breeding, Guangzhou 510640, China; chenwei@gdaas.cn
[4] Anhui Provincial Key Laboratory of Animal Nutritional Regulation and Health, Chuzhou 233100, China
* Correspondence: jineh@ahstu.edu.cn

Abstract

Hericium erinaceus polysaccharide-rich extract (HEP) is obtained from the fruiting bodies and fermented mycelia of *Hericium erinaceus*. It is primarily composed of galactose and glucose, with minor amounts of mannose and fucose, and exhibits immunomodulatory, anti-inflammatory, and antioxidant properties. Heat stress is a major constraint on broiler production, and effective nutritional interventions are needed. However, the effects of HEP on heat-stressed broilers, particularly its regulatory role in immune cell proliferation, apoptosis, and autophagy, remain poorly understood. Therefore, this study aimed to investigate the effects of dietary HEP supplementation on growth performance, immune function, antioxidant capacity, and immune cell proliferation-, apoptosis-, and autophagy-related markers in heat-stressed broilers. A total of 540 21-day-old broilers were randomly allocated into a normal control group (21 ± 1 °C), a heat stress group (33 ± 2 °C, 12 h/day), and four HEP-supplemented groups (0.4, 0.8, 1.2, and 1.6 g/kg diet), which were reared under identical heat stress conditions for 14 days (following a 7-day pre-adaptation period). The results showed that HEP supplementation improved growth performance to varying degrees. Compared with the HSG, the T3 and T4 groups exhibited increases in average daily gain (ADG) of 87.2% and 98.7%, respectively, accompanied by reductions in the feed-to-gain ratio (F/G) of 30.8% and 35.0%, respectively ($p < 0.05$). In immune organs, HEP supplementation improved antioxidant status, as evidenced by increased activities of antioxidant enzymes and total antioxidant capacity, together with reduced malondialdehyde (MDA) content ($p < 0.05$). Notably, MDA content in the thymus decreased by 71.0% in the T4 group compared with the HSG. HEP supplementation also reduced the levels of pro-inflammatory cytokines, including IL-1β and TNF-α, and improved the histological parameters of the thymus, spleen, and bursa of Fabricius in heat-stressed broilers. Additionally, HEP supplementation altered the mRNA expression of genes associated with cell proliferation (PCNA), apoptosis (caspase-3), and autophagy (BECN1, LC3B, and ATG5), accompanied by corresponding changes in immunohistochemical and immunofluorescence staining in immune organs. The present study demonstrates that HEP supplementation may alleviate heat stress-induced impairment of immune function in broilers by enhancing

Check for updates

Academic Editor: Evangelos Zoidis

Received: 10 October 2026
Revised: 21 November 2026
Accepted: 22 November 2026
Published: 25 November 2026

Copyright: © 2026 by the authors. Licensee MDPI, Basel, Switzerland. This article is an open access article distributed under the terms and conditions of the Creative Commons Attribution (CC BY) license.

immune and antioxidant responses; modulating markers associated with cell proliferation, apoptosis, and autophagy; and improving the histological structure of immune organs.

Keywords: *Hericium erinaceus* polysaccharide-rich extract; heat stress; broiler chickens; cell proliferation and apoptosis; immune-antioxidant function; microstructure

1. Introduction

Global warming has made heat stress a major challenge for livestock production, particularly in tropical and subtropical regions [1]. Broilers are especially susceptible to heat stress because their high metabolic rate, lack of sweat glands, and extensive feather coverage limit their heat dissipation capacity [2,3]. Heat stress reduces growth performance, suppresses immune function, impairs antioxidant capacity, and compromises meat quality, causing substantial economic losses [4–6]. It also disrupts intestinal function and cellular turnover, including the balance of cell proliferation, apoptosis, and autophagy [7]. In antibiotic-reduced production systems, plant extracts and natural polysaccharides have attracted attention as nutritional strategies for mitigating heat stress [8]. Natural polysaccharides are biological macromolecules with various biological activities, including antioxidant, immunomodulatory, antihypertensive, antitumor, radioprotective, and anti-aging activities [9]. For example, saffron (Crocus sativus) petal extract improved growth performance, antioxidant status, and immune responses in heat-stressed broilers [10]. *Enteromorpha prolifera* polysaccharides also alleviated growth and intestinal-barrier impairment and modulated the cecal microbiota in heat-stressed yellow-feathered broilers [11]. Collectively, these findings support the use of natural polysaccharides and plant extracts as nutritional strategies to improve antioxidant capacity and stress resistance in livestock and poultry.

Hericium erinaceus is an edible and medicinal fungus of the genus Hericium. It occurs in broad-leaved and mixed forests across temperate regions, including Eastern Europe, Oceania, North America, and East Asia [12]. Its fruiting bodies can be collected or cultivated, whereas its mycelia are commonly produced by submerged fermentation. *Hericium erinaceus* contains glycoproteins, polysaccharides, sterols, and other metabolites associated with intestinal, immunomodulatory, antioxidant, anti-inflammatory, and anti-fatigue activities [13]. *Hericium erinaceus* polysaccharide-rich extract (HEP), obtained from fruiting bodies or fermented mycelia, is a major bioactive macromolecular fraction. Reported activities include stimulation of nerve growth factor synthesis, gastric mucosal protection, and antioxidant, anti-inflammatory, and immunomodulatory effects [14]. Furthermore, *Hericium erinaceus* polysaccharide has been reported to affect cellular processes such as apoptosis and autophagy in animal cells, thereby promoting organ growth and development [15]. Han et al. demonstrated, using a cyclophosphamide-induced immunosuppressed mouse model, that *Hericium erinaceus* polysaccharide downregulated *caspase-3* mRNA expression and upregulated *PCNA* mRNA expression, thereby reducing apoptosis in thymus and spleen tissues [15]. *Hericium erinaceus* polysaccharide also protected IPEC-J2 cells against H_2O_2-induced oxidative injury through mitochondrial and death-receptor pathways [16]. In addition to the effects observed in mammalian immune cells, HEP has been shown to exert immunomodulatory functions in avian species. Prophylactic HEP administration modulated serum cytokines and hormones, alleviated pathological changes caused by Muscovy duck reovirus, and reduced mortality [17]. HEP also improved uterine integrity and eggshell quality in laying hens while altering the uterine microbiota and the expression of biomineralization proteins [18]. At the mechanistic level, genomic and multi-omics analyses of *Hericium erinaceus* have identified carbohydrate-metabolism modules and candidate pathways involved in *Hericium erinaceus* polysaccharide biosynthesis [19]. Structure–function

studies of β-(1→3)-glucans derived from *Hericium erinaceus* further show that their branching ratio and molecular weight differentially affect gut microbiota and short-chain fatty acid (SCFA) production [20]. These findings highlight the need to link HEP composition and structure to its biological effects.

Despite its reported immunomodulatory and antioxidant activities, the effects of HEP on heat-stressed broilers remain poorly defined, and its influence on growth performance, antioxidant status in immune organs, cytokine profiles, and cellular turnover has not been systematically evaluated. Therefore, the present study aimed to evaluate the efficacy of HEP in alleviating heat stress-induced immune impairment in broilers and to determine whether these effects were accompanied by changes in markers of cell proliferation, apoptosis, and autophagy. It was hypothesized that dietary HEP supplementation would improve growth performance and attenuate heat stress-induced immune and antioxidant impairment; that these effects would be accompanied by changes in PCNA-, caspase-3-, and autophagy-related markers; and that these responses would differ among the HEP supplementation levels tested. The findings are expected to provide theoretical and practical support for the use of HEP as a functional feed additive in poultry production.

2. Materials and Methods

2.1. Animal Ethics

The experimental protocol and sample collection were carried out in accordance with the regulations on the Administration of Laboratory Animals promulgated by the National Science and Technology Commission of the People's Republic of China. And the experiment was approved by the Committee of the College of Animal Science, Anhui Science and Technology University, Chuzhou, China (approval no. 2024217; approval date: 17 February 2024).

2.2. Preparation of HEP

The *Hericium erinaceus* powder was purchased from Xi'an Quanao Biotechnology Co., Ltd. (Xi'an, China). The dried powder was ground and passed through an 80-mesh sieve. HEP was extracted by hot water extraction as described previously, with minor modifications [21,22]. In brief, the pretreated powder was extracted with distilled water at a solid-to-liquid ratio of 1:20 (g/mL) in a water bath at 94 °C for 2 h. After extraction, the mixture was cooled to room temperature and centrifuged at 4000× *g* for 15 min at 4 °C. The supernatant was collected, and the extraction was repeated twice. The combined extracts were filtered, concentrated under reduced pressure at 50 °C, and freeze-dried to obtain the crude HEP. The yield of crude HEP was 8.30%. The polysaccharide content of crude HEP was 51.23%, as determined by the phenol–sulfuric acid method using glucose as the standard, with crude protein, crude ash, and crude fat accounting for 21.82%, 0.26%, and 12.85%, respectively. Thus, crude HEP represents a partially purified extract rather than a chromatographically purified polysaccharide fraction. Total polysaccharide content was determined by the phenol–sulfuric acid method using D-glucose as the standard, with absorbance measured at 490 nm. The relative molecular mass was determined by high-performance gel permeation chromatography (HPGPC; Agilent 1260, RID) using Ultrahydrogel™ 2000 and 250 columns maintained at 30 °C, with 0.1 mol/L $NaNO_3$ as the mobile phase at a flow rate of 0.6 mL/min. T-series dextran standards were used for molecular mass calibration. For monosaccharide composition analysis, HEP was hydrolyzed with 2 mol/L trifluoroacetic acid (TFA) at 110 °C for 3 h. The hydrolysate was subsequently derivatized with BSTFA–pyridine at 80 °C for 30 min and analyzed by gas chromatography–mass spectrometry (GC–MS) using an HP-5 column (30 m × 0.32 mm × 0.25 μm), with helium as the carrier gas at a flow rate of 1 mL/min. The oven temperature was programmed from 100 °C to

240 °C. Monosaccharides were identified by comparison with authentic standards, and their relative molar proportions were calculated by area normalization. Using these methods, the relative molecular mass of HEP was determined to be 15.9 kDa. HEP was composed of fucose (9.07%), galactose (30.72%), glucose (54.74%), ribose (1.84%), and mannose (1.76%), with a molar ratio of Glc/Gal/Fuc/Rib/Man = 31.10:17.45:5.15:1.05:1.00.

2.3. Experimental Design, Animals, and Management

A total of 540 21-day-old Abel Akros white-feathered broiler chickens (half of them were male and half were female) were purchased. These chickens were sourced from Bengbu Yiyao Agricultural Technology Development Co., Ltd. (Bengbu, China). Male and female birds were distributed equally within each pen and across all six dietary treatments (approximately 1:1 male/female ratio in every pen and group). After a 7-day acclimation period, the broilers were randomly assigned to 6 groups: the normal control group (CON), the heat stress group (HSG), and four treatment groups (T1–T4). Each group consisted of 6 pens, with 15 broilers per pen. Broilers were housed in their respective pens (100 cm × 90 cm × 38 cm) for the 14-day experimental period. Each pen was placed in an individual independent climate-controlled room. A total of 6 independent rooms were used for the thermoneutral condition (CON), and 30 independent rooms were used for the heat stress condition (HSG and T1–T4, 6 rooms per group). Temperature and relative humidity were individually monitored in each room throughout the experiment. During the entire experiment period, they had free access to feed and water. The basal diet (Table S1) for broiler chickens was formulated in accordance with the China National Feeding Standard of Chicken (GB/T 5916-2008) to meet the nutrient requirements [23]. All groups were fed with basic feed, and the four treatment groups (T1, T2, T3, and T4) were added as 0.4 g/kg, 0.8 g/kg, 1.2 g/kg, and 1.6 g/kg of HEP to the basic feed, respectively. The addition amount of HEP was referenced from previous studies and modified to some extent based on a preliminary experiment conducted before this study [24,25]. Heat stress was applied daily from 09:00 to 21:00 following a published protocol [26]. Room temperature was raised to 33 ± 2 °C and maintained for 12 h, then lowered to 22 ± 1 °C until the next cycle. Humidity was controlled at 60 ± 5% using mist spraying. The CON was kept continuously at 21 ± 1 °C and 60 ± 5% relative humidity. Lighting was provided by combined natural and artificial sources. No mortality occurred during the 14-day experimental period, so no adjustment was required for the growth performance data. The complete experimental design is shown in Figure 1.

2.4. Determination of Growth Performance

The experiment started when broilers were 29 days old and lasted for 14 days. On the 1st day (29 days old), the 7th day (35 days old), and the 14th day (42 days old) of the experiment, the feed intake and body weight of each pen in all groups were measured and recorded. Subsequently, we calculated the average daily gain (ADG), average daily feed intake (ADFI), and feed-to-weight ratio (F/G) of the broilers according to the following formula:

$$\text{ADG (g/d)} = (\text{Final weight} - \text{Initial weight})\ \text{(g)}/\text{Number of days (d)};$$

$$\text{ADFI (g/d)} = \text{Total consumption during the experiment (g)}/(\text{Number of days} \times \text{Number of animals})\ \text{(d)};$$

$$\text{F/G} = \text{ADFI (g/d)}/\text{ADG (g/d)}.$$

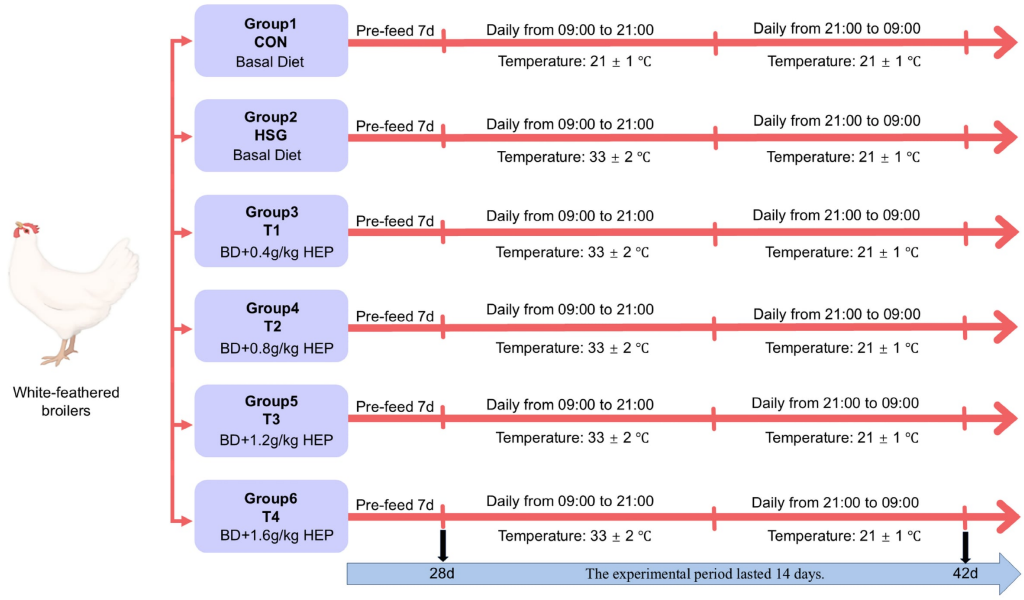

Figure 1. Design of animal experiments. BD = basal diet; HEP = *Hericium erinaceus* polysaccharide-rich extract [27].

2.5. Sample Collection

On the 14th day of the experiment (42-day-old), 6 broilers (half male and half female) from each of the 6 replicate pens in each group were randomly selected, fasted for 12 h (with free access to water), weighed, and euthanized via carotid artery exsanguination. Using sterilized instruments (autoclaved scalpels, surgical scissors, and forceps), the thymus, spleen, and bursa of Fabricius tissues were collected in duplicate. One portion of each tissue was trimmed into 1 cm × 1 cm blocks and preserved in 4% paraformaldehyde solution for histopathological sectioning. The remaining tissue was divided into two aliquots using a sterile blade, placed into RNase-free cryotubes, snap-frozen in liquid nitrogen, and transferred to a −80 °C freezer for subsequent extraction of total RNA and total protein.

2.6. Enzyme-Linked Immunosorbent Assay

Since heat stress induces an inflammatory response in broilers, the levels of interleukin-1β (IL-1β), interleukin-4 (IL-4), and tumor necrosis factor-α (TNF-α) in the thymus, spleen, and bursa of Fabricius were quantified using commercial chicken-specific sandwich ELISA kits (Beijing Dakemei Technology Co., Ltd., Beijing, China) according to the manufacturer's instructions. The kits used were chicken IL-1β (Cat. No. DKM5248A), chicken IL-4 (Cat. No. DKM2667A), and chicken TNF-α (Cat. No. DKM5011A). The intra- and inter-assay coefficients of variation for all kits were <15%, and no significant cross-reactivity with other soluble structural analogs was observed according to the manufacturer.

Tissue samples were thawed, weighed, and homogenized in ice-cold PBS (1:9, *w*/*v*) containing protease inhibitors. Homogenates were centrifuged at 5000× *g* for 10 min at 4 °C, and the supernatants were collected. For the assay, either 50 µL of standards (0, 6.25, 12.5, 25, 50, and 100 pg/mL for TNF-α; 0, 5, 10, 20, 40, and 80 pg/mL for IL-1β) or 10 µL of sample plus 40 µL of sample diluent was added to the pre-coated wells. The plate was sealed and incubated at 37 °C for 30 min. After washing five times, 50 µL of HRP-conjugated detection antibody was added, and the plate was incubated at 37 °C for another 30 min. Wells were washed again, and 50 µL of chromogen solution A and 50 µL of chromogen solution B were added. The plate was incubated at 37 °C for 15 min in the dark. The reaction was stopped with 50 µL of stop solution, and the optical density was measured at 450 nm using a SpectraMax iD3 microplate reader (Molecular Devices, San Jose, CA, USA). Cytokine

concentrations were calculated from the standard curves, with coefficients of determination (R^2) of 0.9912 for IL-1β, 0.9924 for IL-4, and 0.9978 for TNF-α, and they were multiplied by the dilution factor (5×) and normalized to the total protein concentration determined by the BCA method.

2.7. Determination of Antioxidant Capacity

T-AOC, T-SOD activity, GSH-Px activity, and MDA level in the thymus, spleen, and bursa of Fabricius were measured using commercial colorimetric assay kits (Nanjing Jiancheng Bioengineering Institute, Nanjing, China) according to the manufacturer's instructions. The kits used were as follows: T-AOC (FRAP method, based on the reduction of the Fe^{3+}–TPTZ complex, measured at 520 nm), T-SOD (hydroxylamine method, based on the inhibition of superoxide anion-mediated nitrite formation, measured at 550 nm), GSH-Px (colorimetric method, measured at 412 nm), and MDA (TBA method, based on the formation of a red MDA–TBA adduct, measured at 532 nm).

In brief, tissue samples were thawed, weighed, and homogenized in ice-cold physiological saline (0.9%, *w*/*v*) at a ratio of 1:9. Homogenates were centrifuged at 5000 rpm for 10 min at 4 °C, and the supernatants were collected for immediate assay. For T-AOC, 5 μL of supernatant was mixed with 180 μL of working reagent, and the absorbance was recorded at 520 nm after incubation at 37 °C for 5 min. For T-SOD, 0.05 mL of supernatant was mixed with 3.3 mL of reagent, and the absorbance was measured at 550 nm after incubation at 37 °C for 40 min. For GSH-Px, 0.2 mL of supernatant was mixed with 2.5 mL of reagent, and the absorbance was measured at 412 nm after incubation at 37 °C for 15 min. For MDA, 0.1 mL of supernatant was mixed with 4 mL of TBA reagent, incubated at 95 °C for 40 min, cooled, and centrifuged, and the absorbance of the supernatant was measured at 532 nm. Absorbance for T-SOD, GSH-Px, and MDA was measured using a Shimadzu UV-1900i Plus spectrophotometer (Shimadzu, Kyoto, Japan) with 1 cm path-length cuvettes; T-AOC absorbance was measured using a SpectraMax iD3 microplate reader (Molecular Devices, USA). Total protein concentration was determined by the BCA method for normalization.

2.8. Histological Analysis

Fixed spleen, thymus, and bursa of Fabricius samples were processed routinely for paraffin embedding. Briefly, tissues were dehydrated through a graded ethanol series, cleared in xylene, and embedded in paraffin. Sections (5 μm) were cut using a rotary microtome and mounted on glass slides.

For hematoxylin and eosin staining, sections were deparaffinized, rehydrated, and stained following standard protocols [28]. Nuclei were stained with hematoxylin, and cytoplasm was counterstained with eosin. After dehydration and clearing, sections were sealed with neutral gum and a coverslip. For histological morphometric analysis, five representative HE-stained sections from immune organ were used to allow Motic DSAssistant (Motic (Xiamen) Medical Diagnostic Systems Co., Ltd., Xiamen, China) to take photos of the upper, middle, lower, left and right non-overlapping fields of view in the entire tissue area under the same magnification and analyzed using ImageJ software (version 1.54f; National Institutes of Health, Bethesda, MD, USA). The cortical-to-medullary area ratio of the thymus, the area of splenic nodules, and the area of bursal follicles were determined by manually outlining the corresponding structures based on their distinct histological characteristics. The cortical-to-medullary area ratio was calculated as the cortical area divided by the medullary area.

2.9. Immunohistochemistry

Three sections of each immune organ were used for immunohistochemical staining. After deparaffinization, rehydration, and antigen retrieval in citrate buffer (microwave heating, 15 min), endogenous peroxidase activity was blocked with 3% H_2O_2. Sections were blocked with 10% normal goat serum and then incubated overnight at 4 °C with primary antibodies against proliferating cell nuclear antigen (PCNA) (1:200), cleaved cysteinyl aspartate-specific proteinase-3 (cleaved caspase-3) (1:150), or microtubule-associated protein 1 light chain 3 beta (LC3B) (1:400) (all from Proteintech Group Inc., Wuhan, China). After washing, sections were incubated with biotinylated goat anti-rabbit IgG (H+L) (1:200; Proteintech Group Inc., Wuhan, China) at 37 °C for 2 h, followed by DAB development and hematoxylin counterstaining. Finally, sections were dehydrated, cleared, and mounted with neutral resin. For quantitative immunohistochemical analysis, images were captured under identical microscope settings (including light intensity and exposure time) across all sections. We used Motic DSAssistant (Motic (Xiamen) Medical Diagnostic Systems Co., Ltd., Xiamen, China) to take photos of the upper, middle, lower, left and right non-overlapping fields of view in the entire tissue area, carefully avoiding necrotic zones and processing artifacts. The number of positive cells was quantified using ImageJ software (National Institutes of Health, Bethesda, MD, USA).

2.10. Real-Time Quantitative PCR Analysis (RT-PCR)

Total RNA was extracted from the thymus, spleen, and bursa of Fabricius tissues using a spin column-based Total RNA Extraction Kit for Animal Tissues (Tiangen Biotech Co., Ltd., Beijing, China) according to the manufacturer's instructions. RNA purity and concentration were assessed using a NanoDrop spectrophotometer (Thermo Fisher Scientific, Waltham, MA, USA), and RNA integrity was verified by 1% agarose gel electrophoresis. cDNA was synthesized from 1 μg of total RNA using a reverse transcription kit (Vazyme, Nanjing, China) following the manufacturer's protocol. Quantitative real-time PCR (qPCR) was performed using TB Green Premix Ex Taq (Takara Bio Inc., Otsu, Japan) on a QuantStudio 5 Real-Time PCR System (Applied Biosystems, Foster City, CA, USA).

Each reaction (20 μL) contained 10 μL of TB Green Premix Ex Taq, 0.4 μL of each forward and reverse primer (10 μmol/L), 2 μL of cDNA template, and 7.2 μL of nuclease-free water. The thermal cycling conditions were as follows: initial denaturation at 95 °C for 30 s; 40 cycles of 95 °C for 5 s and 60 °C for 30 s; and melting curve analysis from 60 °C to 95 °C to confirm amplification specificity. All samples were run in triplicate (three technical replicates), and the mean Ct value was used for calculation. No-template controls were included in each run to exclude contamination. Primer sequences for all target genes are provided in Table S2.

The amplification efficiency of each primer pair was determined using a standard curve generated from a 10-fold serial dilution of pooled cDNA (five dilution points, from 1:1 to $1:10^4$). The amplification efficiencies were 98.09% for BECN1, 96.75% for LC3B, 98.79% for PCNA, 99.19% for caspase-3, 99.89% for ATG5, and 98.49% for GAPDH, all of which were within the acceptable range of 90–110% and had $R^2 > 0.99$. The specificity of each primer pair was confirmed by the presence of a single peak in the melting curve analysis and by the observation of a single band of the expected size via 2% agarose gel electrophoresis. The relative mRNA expression levels were calculated using the $2^{-\Delta\Delta Ct}$ method, with GAPDH as the internal reference gene.

2.11. Immunofluorescence

Three sections of each immune organ were used for immunofluorescence staining to detect the distribution and expression of PCNA, caspase-3, and LC3B in the thymus, spleen,

and bursa of Fabricius tissues. After deparaffinization and antigen retrieval following the same procedure as used for immunohistochemistry, sections were incubated overnight at 4 °C with primary antibodies (PCNA, 1:200; caspase-3, 1:150; LC3B, 1:400; all from Proteintech Group, Wuhan, China). After washing in PBS, sections were incubated with appropriate secondary antibodies at 37 °C for 2 h. Nuclei were counterstained with DAPI, and sections were mounted with anti-fade medium. For quantitative immunofluorescence analysis, images were captured under a fluorescence microscope using the same laser intensity, exposure time, and gain settings across all experimental groups to ensure comparability. We used Motic DSAssistant (Motic (Xiamen) Medical Diagnostic Systems Co., Ltd., Xiamen, China) to take photos of the upper, middle, lower, left and right non-overlapping fields of view in the entire tissue area, avoiding necrotic areas and artifacts. The acquired images were processed with ImageJ software (version 1.54f; National Institutes of Health, Bethesda, MD, USA). The results were expressed as the average optical density (AOD), calculated as the corrected integrated optical density (IOD) divided by the ROI area (AOD = corrected IOD/area).

2.12. Statistical Analysis

All data were analyzed using IBM SPSS Statistics 27.0 (IBM Corp., Chicago, IL, USA). For growth performance parameters, including ADG, ADFI, and F/G, data were summarized at the pen level ($n = 6$ pens per group, 15 birds per pen) and analyzed using one-way analysis of variance (ANOVA), with treatment as the fixed effect. Sex was therefore not retained as a separate fixed effect, and pen-level means represent pooled data from male and female birds within each pen. Dose–response relationships among the five HEP-supplemented groups (0, 0.4, 0.8, 1.2, and 1.6 g/kg diet, i.e., HSG and T1–T4) were assessed using orthogonal polynomial contrasts, with linear and quadratic contrasts tested for HEP supplementation level. The CON was not included in the dose–response analysis because it was not part of the heat-stress dose series.

For antioxidant capacity, immune-related parameters, gene expression, immunohistochemistry, and immunofluorescence data, linear mixed-effects models (LMMs) were fitted. The random-intercept model accounted for the non-independence among broilers sampled from the same pen and partitioned the total variation into between-pen and within-pen components, thereby providing appropriate standard errors and statistical inference for treatment effects while accounting for the hierarchical structure of the experimental design. Thus, although individual broiler-level measurements were retained in the LMM, treatment effects were inferred based on pen-level replication. Sex was not recorded at the individual sample level; therefore, sex could not be included as a fixed effect in the LMM.

Prior to statistical analyses, the assumptions of normality and homogeneity of variance were assessed on the model residuals rather than on raw data. For one-way ANOVA, these assumptions were tested using the Kolmogorov–Smirnov test with Lilliefors correction and Levene's test, respectively. For LMMs, normality of residuals was checked using quantile–quantile (Q–Q) plots and the Shapiro–Wilk test, while homogeneity of variance was verified by visually inspecting standardized residuals against fitted values. When a significant overall treatment effect was detected ($p < 0.05$), multiple comparisons among estimated marginal means were performed using Dunnett-adjusted tests. Two sets of comparisons were conducted: (1) comparisons of HSG and all HEP-supplemented groups (T1–T4) against the thermoneutral control group (CON), and (2) comparisons of CON and all HEP-supplemented groups (T1–T4) against the heat-stressed control group (HSG). These comparisons were used to evaluate the effects of heat stress and the efficacy of HEP supplementation in mitigating heat stress-induced alterations.

Results are presented as means ± standard error (SE) of estimated marginal means. For mixed-model analyses, SE values were derived from the residual variance component of the fitted model. Statistical significance was declared at $p < 0.05$, whereas $p < 0.01$ was considered highly significant.

For graphical and tabular presentation, a dual-annotation system was used. Asterisks (* and **) indicate significant differences compared with the CON based on Dunnett-adjusted comparisons (* $p < 0.05$, ** $p < 0.01$). Hash symbols (# and ##) indicate significant differences compared with the HSG based on Dunnett-adjusted comparisons (# $p < 0.05$, ## $p < 0.01$). All symbols and comparison references are clearly defined in figure legends and table footnotes.

3. Results

3.1. Effects of HEP on Growth Performance

On day 14 of the experiment, heat stress significantly reduced ADG and ADFI by 53.8% and 30.9%, respectively, while increasing the F/G ratio by 49.4% compared with the CON ($p < 0.05$; Table 1). Dietary HEP supplementation improved growth performance in heat-stressed broilers. Compared with the HSG, ADG increased by 30.4%, 43.3%, 87.2%, and 98.7% in the T1, T2, T3, and T4 groups, respectively, while ADFI increased by 19.3%, 21.7%, 29.8%, and 29.1%, respectively. Notably, the T3 and T4 groups exhibited significantly higher ADG and ADFI values than the HSG ($p < 0.05$). Furthermore, the F/G ratio decreased by 8.5%, 15.0%, 30.8%, and 35.0% in the T1, T2, T3, and T4 groups, respectively, with significantly lower values observed in the T3 and T4 groups compared with the HSG ($p < 0.05$).

Table 1. Effects of *Hericium erinaceus* polysaccharide-rich extract on the production performance of heat-stressed broilers.

Item	Groups						SEM	*p*-Value		
	CON	HSG	T1	T2	T3	T4		Treatment	Linear	Quadratic
ADG (g/day)	60.71 #	28.04 *	36.57 *	40.18 *	52.50 #	55.71 #	2.927	0.024	0.012	0.971
ADFI (g/day)	105.51 #	72.92 *	86.96 *	88.73 *	94.63 #	94.16 #	2.258	0.048	0.146	0.785
F/G ratio	1.74 #	2.60 *	2.38 *	2.21 *	1.80 #	1.69 #	0.071	0.017	<0.001	0.765

Note: ADG = average daily gain. ADFI = average daily feed intake. F/G = feed-to-gain ratio. SEM = standard error of the mean. CON = fed basal diet under thermoneutral conditions. HSG = fed basal diet under heat stress. T1 = fed basal diet with 0.4 g/kg HEP under heat stress. T2 = fed basal diet with 0.8 g/kg HEP under heat stress. T3 = fed basal diet with 1.2 g/kg HEP under heat stress. T4 = fed basal diet with 1.6 g/kg HEP under heat stress. Post hoc comparisons were performed using Dunnett's multiple comparison test to control the family-wise error rate. * Means that indicate significant differences between the HSG and T1–T4 compared to the CON (* $p < 0.05$). # Means that indicate significant differences between the CON and T1–T4 compared to the HSG (# $p < 0.05$). Values without any superscript symbol indicate no significant difference from either the CON or HSG ($p > 0.05$). Results are means ± SEM ($n = 6$ pens/treatment, with 15 birds per pen. The pen was considered the experimental unit used for statistical analysis).

3.2. Effects of HEP on Immune Factor Levels

On day 14 of the experiment, heat stress increased the concentrations of IL-1β, IL-4, and TNF-α in the thymus by 13.0%, 42.8%, and 11.3%, respectively, compared with the CON ($p < 0.05$ or $p < 0.01$; Table 2). Dietary HEP supplementation reduced these inflammatory cytokine concentrations compared with the HSG. Specifically, thymic IL-1β concentrations decreased by 12.0%, 16.5%, and 12.5% in the T2, T3, and T4 groups, respectively ($p < 0.05$ or $p < 0.01$). Thymic IL-4 and TNF-α concentrations decreased by 10.2–31.9% and 8.6–25.3%, respectively, in the HEP-supplemented groups (T1–T4; $p < 0.05$ or $p < 0.01$). In the spleen, heat stress increased IL-1β and TNF-α concentra-

tions by 6.3% and 16.6%, respectively, compared with the CON ($p < 0.01$). Compared with the HSG, splenic IL-1β concentration was reduced by 5.8% in the T4 group ($p < 0.01$), whereas TNF-α concentrations decreased by 12.8% and 22.2% in the T2 and T4 groups, respectively ($p < 0.01$). In the bursa of Fabricius, heat stress increased IL-1β and TNF-α concentrations by 40.7% and 18.6%, respectively, compared with the CON ($p < 0.01$). Dietary HEP supplementation reduced IL-1β concentrations by 11.9%, 12.0%, 16.8%, and 26.7% in the T1, T2, T3, and T4 groups, respectively, compared with the HSG ($p < 0.01$). Similarly, TNF-α concentrations decreased by 17.9% and 32.1% in the T3 and T4 groups, respectively ($p < 0.01$).

Table 2. Effects of *Hericium erinaceus* polysaccharide-rich extract on cytokine concentration in the immune organs of heat-stressed broilers.

Item	Groups						SE (EMMs)	F (df1, df2)	*p*-Value
	CON	HSG	T1	T2	T3	T4			
Thymus									
IL-1β (pg/mL)	98.76 $^{\#}$	111.59 *	108.57	98.22 $^{\#}$	93.17 $^{\#\#}$	97.69 $^{\#}$	3.761	3.617 (5, 30)	0.011
IL-4 (pg/mL)	17.63 $^{\#\#}$	25.17 **	22.61 $^{**\#\#}$	19.58 $^{*\#\#}$	19.68 $^{*\#\#}$	17.13 $^{\#\#}$	0.595	25.602 (5, 30)	<0.001
TNF-α (pg/mL)	12.66 $^{\#}$	14.09 *	12.88 $^{\#}$	11.20 $^{*\#\#}$	11.51 $^{\#\#}$	10.52 $^{**\#\#}$	0.405	10.390 (5, 30)	<0.001
Spleen									
IL-1β (pg/mL)	97.16 $^{\#\#}$	103.25 **	109.28 $^{**\#\#}$	104.38 **	104.77 **	97.21 $^{\#\#}$	1.133	17.348 (5, 30)	<0.001
IL-4 (pg/mL)	21.00	24.98	23.61	22.83	22.73	22.22	0.903	2.195 (5, 30)	0.081
TNF-α (pg/mL)	11.51 $^{\#\#}$	13.42 **	12.66	11.70 $^{\#\#}$	12.88 *	10.44 $^{\#\#}$	0.438	6.194 (5, 30)	<0.001
Bursa of Fabricius									
IL-1β (pg/mL)	92.11 $^{\#\#}$	129.59 **	114.14 $^{**\#\#}$	114.06 $^{**\#\#}$	107.81 $^{**\#\#}$	94.93 $^{\#\#}$	2.087	46.466 (5, 30)	<0.001
IL-4 (pg/mL)	22.83	23.55	24.98	23.58	22.83	21.75	0.867	1.216 (5, 30)	0.326
TNF-α (pg/mL)	15.62 $^{\#\#}$	18.52 **	18.57 **	17.72 *	15.20 $^{\#\#}$	12.57 $^{**\#\#}$	0.633	13.745 (5, 30)	<0.001

Note: IL-1β = interleukin-1β. IL-4 = interleukin-4. TNF-α = tumor necrosis factor-α. SE = standard error of estimated marginal means (EMMs). CON = fed basal diet under thermoneutral conditions. HSG = fed basal diet under heat stress. T1 = fed basal diet with 0.4 g/kg HEP under heat stress. T2 = fed basal diet with 0.8 g/kg HEP under heat stress. T3 = fed basal diet with 1.2 g/kg HEP under heat stress. T4 = fed basal diet with 1.6 g/kg HEP under heat stress. Post hoc multiple comparisons versus CON were performed using Dunnett's test based on EMMs (* $p < 0.05$, ** $p < 0.01$). Post hoc multiple comparisons versus HSG were performed using Dunnett's test based on EMMs ($^{\#}$ $p < 0.05$, $^{\#\#}$ $p < 0.01$). Values without any superscript symbol indicate no significant difference from either the CON or HSG ($p > 0.05$). Values are presented as estimated marginal means (EMMs) ± standard error (SE) based on a linear mixed model (LMM), with pen considered as a random effect. The pen was the experimental unit ($n = 6$ pens/treatment). There were 6 replicates (pens) per treatment, with 6 birds sampled per pen (36 birds per treatment).

3.3. Effects of HEP on Antioxidant Function

On day 14 of the experiment, heat stress significantly decreased thymic T-SOD activity, GSH-Px activity, and T-AOC by 24.7%, 34.4%, and 14.2%, respectively, while increasing MDA levels by 245.0% compared with the CON ($p < 0.01$; Table 3). Compared with the HSG, dietary HEP supplementation significantly increased T-SOD activity by 31.9% in the T4 group ($p < 0.01$) and GSH-Px activity by 18.4% and 30.0% in the T3 and T4 groups, respectively ($p < 0.05$ or $p < 0.01$). Thymic T-AOC increased by 18.5% in the T4 group ($p < 0.01$). In addition, MDA levels decreased by 60.9%, 53.6%, 72.5%, and 71.0% in the T1, T2, T3, and T4 groups, respectively ($p < 0.01$). In the spleen, heat stress significantly decreased T-SOD activity, GSH-Px activity, and T-AOC by 32.7%, 20.3%, and 26.0%, respectively, while increasing MDA levels by 43.0% compared with the CON ($p < 0.05$ or $p < 0.01$). Compared with the HSG, T-SOD activity increased by 30.0%, 16.6%, 40.0%, and 48.6% in the T1, T2, T3, and T4 groups, respectively ($p < 0.05$ or $p < 0.01$). GSH-Px activity increased by 25.5% in the T4 group ($p < 0.01$), whereas T-AOC increased by 24.3% and 43.2% in the T3 and T4 groups, respectively ($p < 0.05$ or $p < 0.01$). Furthermore, MDA levels decreased by 25.6% in the T4 group ($p < 0.05$). In the bursa of Fabricius, heat stress significantly decreased T-SOD activity, GSH-Px activity, and T-AOC by 34.0%, 50.3%, and 29.2%, respectively, while

increasing MDA levels by 164.5% compared with the CON ($p < 0.01$). Compared with the HSG, T-SOD activity increased by 34.7% in the T4 group ($p < 0.01$). GSH-Px activity increased by 76.4% and 132.9% in the T3 and T4 groups, respectively ($p < 0.01$), while T-AOC increased by 61.8% in the T4 group ($p < 0.01$). Additionally, MDA levels decreased by 70.7% in the T4 group ($p < 0.01$).

Table 3. Effects of *Hericium erinaceus* polysaccharide-rich extract on the antioxidant capacity of immune organs in heat-stressed broilers.

Item	Groups						SE (EMMs)	F (df1, df2)	*p*-Value
	CON	HSG	T1	T2	T3	T4			
Thymus									
T-SOD (U/mgprot)	19.17 $^{\#\#}$	14.44 **	14.87 **	15.53 *	16.62	19.04 $^{\#\#}$	1.087	3.594 (5, 30)	0.009
GSH-Px (U/mgprot)	97.01 $^{\#\#}$	63.68 **	63.15 **	71.98 **	75.41 **$^{\#}$	82.78 **$^{\#\#}$	3.789	11.991 (5, 30)	<0.001
T-AOC (mmol/gprot)	5.30 $^{\#\#}$	4.55 **	4.47 **	4.51 **	4.71 **	5.39 $^{\#\#}$	0.144	8.336 (5, 30)	<0.001
MDA (nmol/mgprot)	0.20 $^{\#\#}$	0.69 **	0.27 $^{\#\#}$	0.32 $^{\#\#}$	0.19 $^{\#\#}$	0.20 $^{\#\#}$	0.052	12.765 (5, 30)	<0.001
Spleen									
T-SOD (U/mgprot)	9.02 $^{\#\#}$	6.07 **	7.89 *$^{\#\#}$	7.08 **$^{\#}$	8.50 $^{\#\#}$	9.02 $^{\#\#}$	0.338	12.108 (5, 30)	<0.001
GSH-Px (U/mgprot)	67.99 $^{\#}$	54.20 *	55.60 *	57.10 *	64.72	68.02 $^{\#\#}$	3.702	3.060 (5, 30)	0.019
T-AOC (mmol/gprot)	0.50 $^{\#\#}$	0.37 **	0.40 *	0.45	0.46 $^{\#}$	0.53 $^{\#\#}$	0.026	4.880 (5, 30)	0.001
MDA (nmol/mgprot)	0.93 $^{\#}$	1.33 *	1.24 *	1.14 *	1.13	0.99 $^{\#}$	0.081	3.699 (5, 30)	0.007
Bursa of Fabricius									
T-SOD (U/mgprot)	59.56 $^{\#\#}$	39.32 **	32.65 **	30.44 **	39.25 **	52.95 $^{\#\#}$	3.446	11.223 (5, 30)	<0.001
GSH-Px (U/mgprot)	70.03 $^{\#\#}$	34.80 **	47.70 **	47.17 **	61.37 $^{\#\#}$	81.06 $^{\#\#}$	4.709	12.981 (5, 30)	<0.001
T-AOC (mmol/gprot)	0.96 $^{\#\#}$	0.68 **	0.69 **	0.78 **	0.79 *	1.10 *$^{\#\#}$	0.047	13.016 (5, 30)	<0.001
MDA (nmol/mgprot)	0.31 $^{\#\#}$	0.82 **	0.48 **	0.48	0.40	0.24 $^{\#\#}$	0.098	4.168 (5, 30)	0.004

Note: T-SOD = total superoxide dismutase. GSH-Px = glutathione peroxidase. T-AOC = total antioxidant capacity. MDA = malondialdehyde. SE = standard error of estimated marginal means (EMMs). CON = fed basal diet under thermoneutral conditions. HSG = fed basal diet under heat stress. T1 = fed basal diet with 0.4 g/kg HEP under heat stress. T2 = fed basal diet with 0.8 g/kg HEP under heat stress. T3 = fed basal diet with 1.2 g/kg HEP under heat stress. T4 = fed basal diet with 1.6 g/kg HEP under heat stress. Post hoc multiple comparisons versus CON were performed using Dunnett's test based on EMMs (* $p < 0.05$, ** $p < 0.01$). Post hoc multiple comparisons versus HSG were performed using Dunnett's test based on EMMs ($^{\#}$ $p < 0.05$, $^{\#\#}$ $p < 0.01$). Values without any superscript symbol indicate no significant difference from either the CON or HSG ($p > 0.05$). Values are presented as estimated marginal means (EMMs) ± standard error (SE) based on a linear mixed model (LMM), with pen considered as a random effect. The pen was the experimental unit ($n = 6$ pens/treatment). There were 6 replicates (pens) per treatment, with 6 birds sampled per pen (36 birds per treatment).

3.4. Effects of HEP on Immune Organ Morphology

Histological examination of the thymus, spleen, and bursa of Fabricius revealed distinct morphological alterations among the treatment groups (Figure 2). In the thymus, the CON exhibited normal architecture, with large and closely arranged thymic lobules, a distinct corticomedullary boundary, and abundant, densely packed thymocytes (Figure 2A). Compared with the CON, the HSG exhibited structural abnormalities, characterized by smaller thymic lobules, increased interlobular connective tissue, a thinner cortex, an enlarged medulla with visible vacuoles, and loosely arranged thymocytes (Figure 2B). Compared with the HSG, the T3 and T4 groups showed structural recovery to varying degrees, as evidenced by tightly arranged thymic lobules, reduced interlobular connective tissue, a clear corticomedullary boundary, a thickened cortex, a smaller medulla with fewer vacuoles, and an increased number of densely packed thymocytes (Figure 2E,F). In the spleen, the CON presented normal architecture, with distinct white pulp structures and numerous, evenly distributed splenic nodules (Figure 2G). Compared with the CON, the HSG exhibited disrupted splenic architecture, characterized by indistinct white pulp structures, reduced numbers and size of splenic nodules, loosely arranged lymphocytes, and increased blood cell infiltration in the red pulp (Figure 2H). Compared with the HSG, the T3 and T4 groups showed a degree of structural recovery, as evidenced by clearer white pulp structures, en-

larged splenic nodules, densely arranged lymphocytes, and reduced blood cell infiltration in the red pulp (Figure 2K,L). In the bursa of Fabricius, the CON showed normal architecture, with larger and more numerous bursal lobules, as well as abundant, closely arranged bursal follicles (Figure 2M). Compared with the CON, the HSG exhibited smaller bursal lobules, significantly reduced numbers and size of bursal follicles, loosely arranged cells, markedly increased interfollicular connective tissue, indistinct corticomedullary boundaries, a reduced number of lymphocytes, and some vacuoles in the medulla (Figure 2N). Compared with the HSG, the T3 and T4 groups showed structural recovery, as evidenced by larger bursal lobules; significantly increased numbers of closely arranged follicles; clearer corticomedullary boundaries; and an increased number of lymphocytes (Figure 2Q,R).

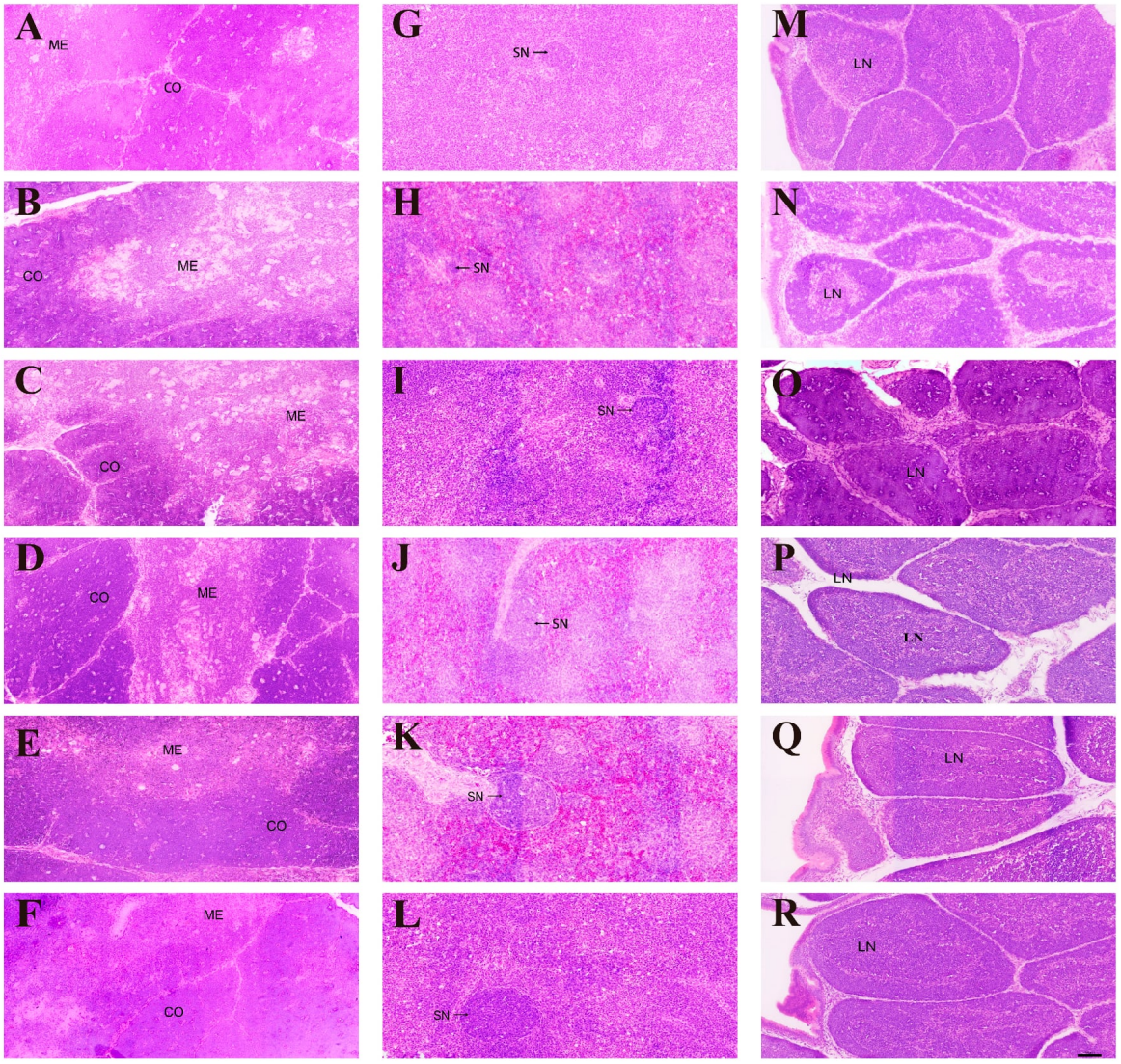

Figure 2. Effect of *Hericium erinaceus* polysaccharide-rich extract on the histological structure of immune organs in heat-stressed broilers. (**A**,**G**,**M**): CON. (**B**,**H**,**N**): HSG. (**C**,**I**,**O**): T1. (**D**,**J**,**P**): T2. (**E**,**K**,**Q**): T3. (**F**,**L**,**R**): T4. (**A**–**F**): representative histological structure of the thymus. (**G**–**L**): representative histological structure of the spleen. (**M**–**R**): representative histological structure of the bursa of Fabricius. CON = fed basal diet under thermoneutral conditions. HSG = fed basal diet under heat stress. T1 = fed basal diet with 0.4 g/kg HEP under heat stress. T2 = fed basal diet with 0.8 g/kg HEP under heat stress. T3 = fed basal diet with 1.2 g/kg HEP under heat stress. T4 = fed basal diet with 1.6 g/kg HEP under heat stress. CO: cortex; ME: medulla; SN: splenic nodule; LN: follicular nodule. Scale bar: 200 μm.

As shown in Table 4, heat stress significantly reduced the thymic cortex-to-medulla ratio by 62.1% compared with the CON ($p < 0.01$). Compared with the HSG, HEP supplementation significantly increased this ratio by 100.0%, 106.8%, 147.3%, and 221.6% in the T1, T2, T3, and T4 groups, respectively ($p < 0.01$). In the spleen, heat stress significantly decreased the splenic nodule area by 18.4% compared with the CON ($p < 0.01$). Compared with the HSG, the splenic nodule area significantly increased by 22.5%, 35.8%, 45.8%, and 47.1% in the T1, T2, T3, and T4 groups, respectively ($p < 0.01$). In the bursa of Fabricius, heat stress significantly reduced the follicular area by 48.8% compared with the CON ($p < 0.01$). Compared with the HSG, the follicular area increased by 57.6%, 91.2%, and 103.2% in the T2, T3, and T4 groups, respectively ($p < 0.01$).

Table 4. Effect of *Hericium erinaceus* polysaccharide-rich extract on histological parameters of immune organs in heat-stressed broilers.

Item	Groups						SE (EMMs)	F (df1, df2)	*p*-Value
	CON	HSG	T1	T2	T3	T4			
Ratio of Thymic Cortex to Medulla	1.95 $^{\#\#}$	0.74 **	1.48 *$^{\#\#}$	1.53 $^{\#\#}$	1.83 $^{\#\#}$	2.38 $^{\#\#}$	0.149	13.680 (5, 30)	<0.001
Area of Splenic Nodules ($10^3\mu m^2$)	5.72 $^{\#\#}$	4.67 **	5.72 $^{\#\#}$	6.34 $^{\#\#}$	6.81 **$^{\#\#}$	6.87 **$^{\#\#}$	0.223	13.905 (5, 30)	<0.001
Area of Bursal Follicles ($10^6\mu m^2$)	4.88 $^{\#\#}$	2.50 **	3.06 **	3.94 *$^{\#\#}$	4.78 $^{\#\#}$	5.08 $^{\#\#}$	0.286	13.910 (5, 30)	<0.001

Note: SE = standard error of estimated marginal means (EMMs). CON = fed basal diet under thermoneutral conditions. HSG = fed basal diet under heat stress. T1 = fed basal diet with 0.4 g/kg HEP under heat stress. T2 = fed basal diet with 0.8 g/kg HEP under heat stress. T3 = fed basal diet with 1.2 g/kg HEP under heat stress. T4 = fed basal diet with 1.6 g/kg HEP under heat stress. Post hoc multiple comparisons versus CON were performed using Dunnett's test based on EMMs (* $p < 0.05$, ** $p < 0.01$). Post hoc multiple comparisons versus HSG were performed using Dunnett's test based on EMMs ($^{\#\#}$ $p < 0.01$). Values without any superscript symbol indicate no significant difference from either the CON or HSG ($p > 0.05$). Values are presented as estimated marginal means (EMMs) ± standard error (SE) based on a linear mixed model (LMM), with pen considered as a random effect. The pen was the experimental unit ($n = 6$ pens/treatment). There were 6 replicates (pens) per treatment, with 6 birds sampled per pen (36 birds per treatment).

3.5. Effects of HEP on the Distribution and Number of Positive Cells for Proliferation-, Apoptosis-, and Autophagy-Related Proteins in Immune Organs

Positive cells were identified by brown staining (Figures 3–5). In the CON, the immunopositive signals for proliferating cell nuclear antigen (PCNA), cysteine-aspartate-specific proteinase-3 (caspase-3), and microtubule-associated protein 1 light chain 3 beta (LC3B) in the thymus, spleen, and bursa of Fabricius exhibited spatially specific distribution patterns. PCNA-positive cells were densely concentrated in the thymic cortex, the white pulp of the spleen (Figure 3), and the follicles of the bursa of Fabricius. Caspase-3-positive cells were predominantly localized in the thymic cortex, the white pulp of the spleen, and the cortico-medullary junction of the bursa of Fabricius (Figure 4). LC3B-positive cells were sparsely distributed throughout the immune organs (Figure 5). In the HSG, the number of PCNA-positive cells was distinctly reduced in all immune organs, particularly in regions typically associated with high proliferative activity. The number of caspase-3-positive cells increased substantially, and their distribution transitioned from a localized to a diffuse pattern. Furthermore, LC3B-positive signals were markedly enhanced. Following HEP supplementation, the number of PCNA-positive cells was significantly increased, especially in the thymic cortex, splenic white pulp, and bursal follicles. The number of caspase-3-positive cells was notably decreased, and their distribution reverted from a diffuse pattern to a more localized and physiologically typical arrangement. Moreover, both the intensity and distribution range of LC3B-positive signals tended to normalize.

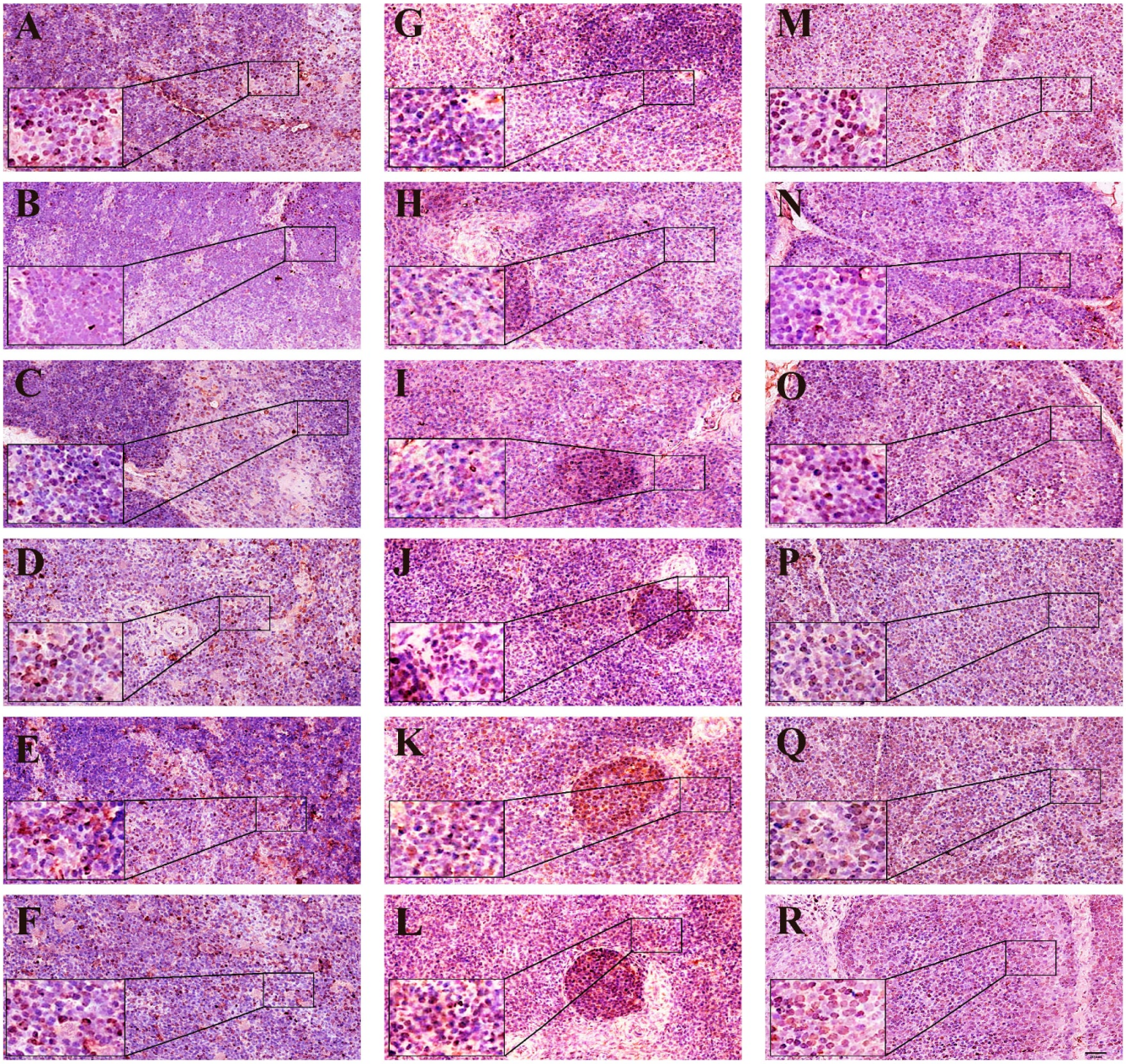

Figure 3. Effects of *Hericium erinaceus* polysaccharide-rich extract on PCNA-positive cells in the immune organs of heat-stressed broilers. (**A**,**G**,**M**): CON. (**B**,**H**,**N**): HSG. (**C**,**I**,**O**): T1. (**D**,**J**,**P**): T2. (**E**,**K**,**Q**): T3. (**F**,**L**,**R**): T4. (**A**–**F**): representative images of PCNA-positive cells in the thymus. (**G**–**L**): representative images of PCNA-positive cells in the spleen. (**M**–**R**): representative images of PCNA-positive cells in the bursa of Fabricius. CON = fed basal diet under thermoneutral conditions. HSG = fed basal diet under heat stress. T1 = fed basal diet with 0.4 g/kg HEP under heat stress. T2 = fed basal diet with 0.8 g/kg HEP under heat stress. T3 = fed basal diet with 1.2 g/kg HEP under heat stress. T4 = fed basal diet with 1.6 g/kg HEP under heat stress. PCNA = proliferating cell nuclear antigen. Scale bar: 80 μm.

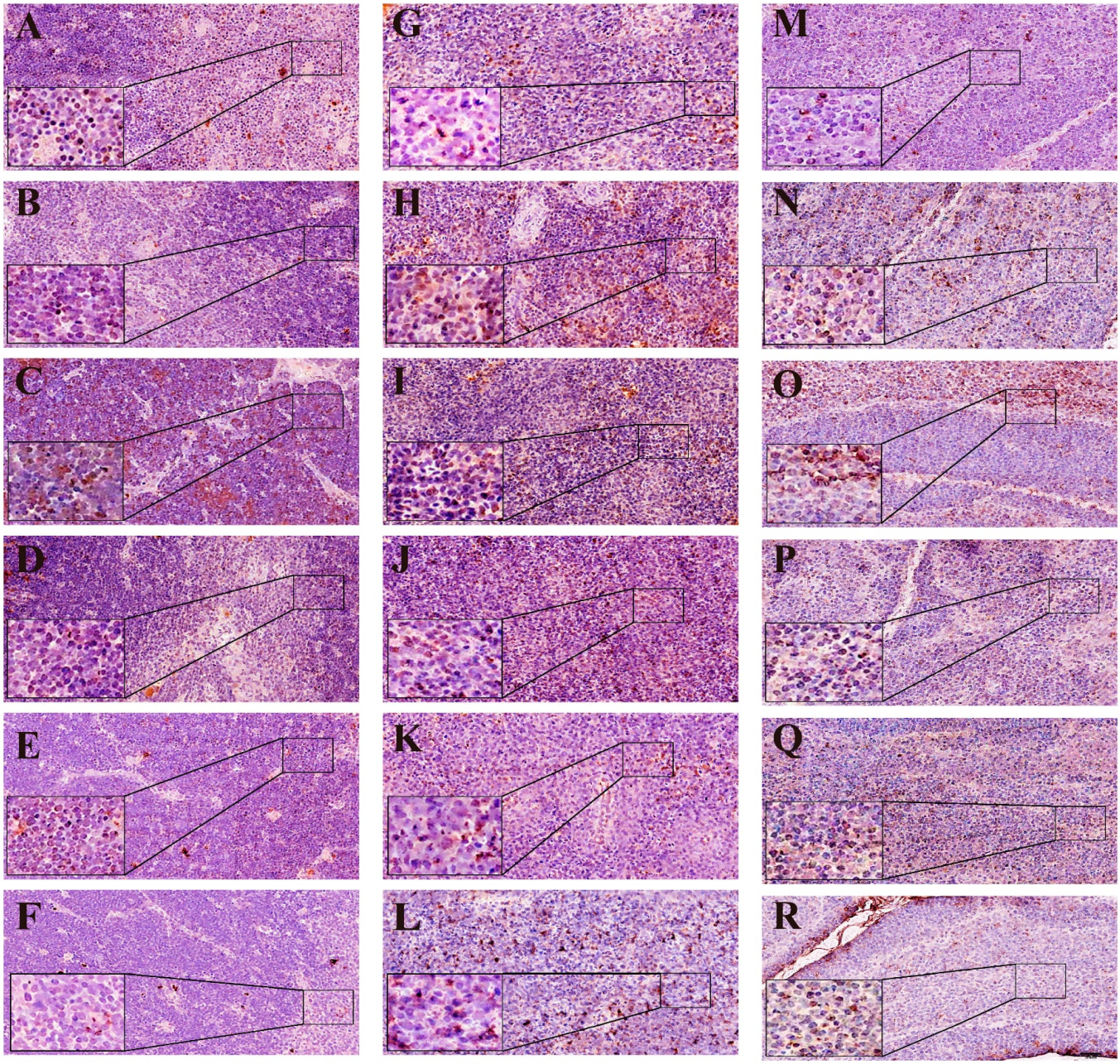

Figure 4. Effects of *Hericium erinaceus* polysaccharide-rich extract on caspase-3-positive cells in the immune organs of heat-stressed broilers. (**A**,**G**,**M**): CON. (**B**,**H**,**N**): HSG. (**C**,**I**,**O**): T1. (**D**,**J**,**P**): T2. (**E**,**K**,**Q**): T3. (**F**,**L**,**R**): T4. (**A**–**F**): representative images of caspase-3-positive cells in the thymus. (**G**–**L**): representative images of caspase-3-positive cells in the spleen. (**M**–**R**): representative images of caspase-3-positive cells in the bursa of Fabricius. CON = fed basal diet under thermoneutral conditions. HSG = fed basal diet under heat stress. T1 = fed basal diet with 0.4 g/kg HEP under heat stress. T2 = fed basal diet with 0.8 g/kg HEP under heat stress. T3 = fed basal diet with 1.2 g/kg HEP under heat stress. T4 = fed basal diet with 1.6 g/kg HEP under heat stress. Caspase-3 = cysteinyl aspartate-specific proteinase-3. Scale bar: 80 μm.

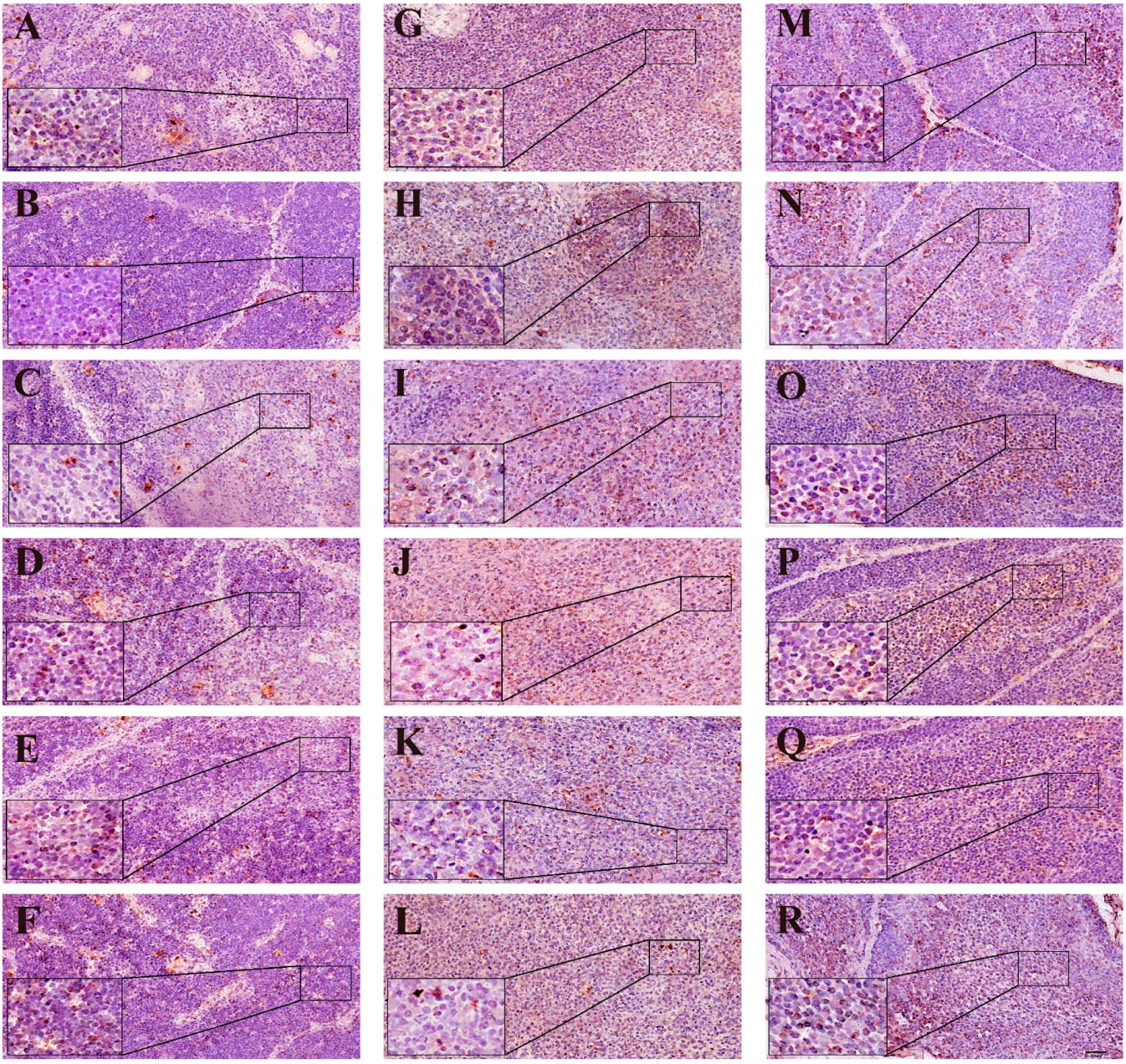

Figure 5. Effects of *Hericium erinaceus* polysaccharide-rich extract on LC3B-positive cells in the immune organs of heat-stressed broilers. (**A**,**G**,**M**): CON. (**B**,**H**,**N**): HSG. (**C**,**I**,**O**): T1. (**D**,**J**,**P**): T2. (**E**,**K**,**Q**): T3. (**F**,**L**,**R**): T4. (**A**–**F**): representative images of LC3B-positive cells in the thymus. (**G**–**L**): representative images of LC3B-positive cells in the spleen. (**M**–**R**): representative images of LC3B-positive cells in the bursa of Fabricius. CON = fed basal diet under thermoneutral conditions. HSG = fed basal diet under heat stress. T1 = fed basal diet with 0.4 g/kg HEP under heat stress. T2 = fed basal diet with 0.8 g/kg HEP under heat stress. T3 = fed basal diet with 1.2 g/kg HEP under heat stress. T4 = fed basal diet with 1.6 g/kg HEP under heat stress. LC3B = microtubule-associated protein 1 light chain 3 beta. Scale bar: 80 μm.

As shown in Table 5, heat stress significantly decreased the number of PCNA-positive cells by 64.7% in the thymus compared with the CON ($p < 0.01$), while increasing the numbers of caspase-3- and LC3B-positive cells by 79.3% and 306.9%, respectively ($p < 0.01$). Compared with the HSG, the numbers of PCNA-positive cells increased by 76.1%, 194.4%, 194.2%, and 202.3% in the T1, T2, T3, and T4 groups, respectively ($p < 0.01$). The numbers of caspase-3-positive cells decreased by 20.5% and 40.3% in the T3 and T4 groups, respectively

($p < 0.01$), whereas the numbers of LC3B-positive cells decreased by 26.6%, 41.5%, 81.5%, and 84.1% in the T1, T2, T3, and T4 groups, respectively ($p < 0.05$ or $p < 0.01$). In the spleen, heat stress significantly decreased the number of PCNA-positive cells by 41.0% compared with the CON ($p < 0.01$), while increasing the numbers of caspase-3- and LC3B-positive cells by 9.0% and 184.2%, respectively ($p < 0.01$). Compared with the HSG, the numbers of PCNA-positive cells increased by 47.6%, 87.6%, 88.9%, and 96.3% in the T1, T2, T3, and T4 groups, respectively ($p < 0.01$). The numbers of caspase-3-positive cells decreased by 3.5% and 7.1% in the T3 and T4 groups, respectively ($p < 0.05$ or $p < 0.01$), while the numbers of LC3B-positive cells decreased by 19.1%, 31.4%, 46.5%, and 56.9% in the T1, T2, T3, and T4 groups, respectively ($p < 0.05$ or $p < 0.01$). In the bursa of Fabricius, heat stress significantly decreased the number of PCNA-positive cells by 18.8% compared with the CON ($p < 0.01$), while increasing the numbers of caspase-3- and LC3B-positive cells by 8.7% and 18.9%, respectively ($p < 0.01$). Compared with the HSG, the numbers of PCNA-positive cells increased by 20.6%, 11.3%, 17.1%, and 19.9% in the T1, T2, T3, and T4 groups, respectively ($p < 0.01$). The numbers of caspase-3-positive cells decreased by 2.9%, 4.4%, and 7.7% in the T2, T3, and T4 groups, respectively ($p < 0.05$ or $p < 0.01$). Additionally, the number of LC3B-positive cells decreased by 39.2% in the T4 group ($p < 0.01$).

Table 5. Effect of *Hericium erinaceus* polysaccharide-rich extract on the numbers of PCNA-, caspase-3-, and LC3B-positive cells in immune organs of heat-stressed broilers.

Item	Groups						SE (EMMs)	F (df1, df2)	*p*-Value
	CON	HSG	T1	T2	T3	T4			
Thymus									
PCNA	1224.44 $^{\#\#}$	431.78 **	760.22 $^{**\#\#}$	1271.11 $^{\#\#}$	1270.45 $^{\#\#}$	1305.11 $^{\#\#}$	38.289	89.894 (5, 30)	<0.001
Caspase-3	159.00 $^{\#\#}$	285.11 **	255.33 **	244.45 **	226.78 $^{**\#\#}$	170.33 $^{\#\#}$	14.277	12.015 (5, 30)	<0.001
LC3B	90.55 $^{\#\#}$	368.45 **	270.34 $^{**\#}$	215.55 $^{**\#\#}$	68.11 $^{\#\#}$	58.78 $^{\#\#}$	31.467	16.188 (5, 30)	<0.001
Spleen									
PCNA	1233.00 $^{\#\#}$	727.56 **	1073.89 $^{\#\#}$	1365.00 $^{\#\#}$	1374.33 $^{\#\#}$	1427.89 $^{*\#\#}$	56.915	21.594 (5, 30)	<0.001
Caspase-3	272.00 $^{\#\#}$	296.44 **	294.56 **	291.33 **	286.00 $^{*\#}$	275.44 $^{\#\#}$	3.586	8.058 (5, 30)	<0.001
LC3B	140.89 $^{\#\#}$	400.45 **	323.89 $^{**\#}$	275.56 $^{**\#\#}$	214.33 $^{*\#\#}$	172.78 $^{\#\#}$	24.437	15.995 (5, 30)	<0.001
Bursa of Fabricius									
PCNA	1280.67 $^{\#\#}$	1040.22 **	1254.11 $^{\#\#}$	1158.11 $^{**\#\#}$	1217.78 $^{\#\#}$	1247.67 $^{\#\#}$	22.174	15.989 (5, 30)	<0.001
Caspase-3	316.89 $^{\#\#}$	344.33 **	343.33 **	334.33 $^{**\#}$	329.22 $^{*\#\#}$	317.67 $^{\#\#}$	3.219	13.910 (5, 30)	<0.001
LC3B	1020.78 $^{\#\#}$	1213.67 **	1184.44 *	1140.22	1114.33	737.33 $^{**\#\#}$	49.157	12.722 (5, 30)	<0.001

Note: PCNA = proliferating cell nuclear antigen. Caspase-3 = cysteinyl aspartate-specific proteinase-3. LC3B = microtubule-associated protein 1 light chain 3 beta. SE = standard error of estimated marginal means (EMMs). CON = fed basal diet under thermoneutral conditions. HSG = fed basal diet under heat stress. T1 = fed basal diet with 0.4 g/kg HEP under heat stress. T2 = fed basal diet with 0.8 g/kg HEP under heat stress. T3 = fed basal diet with 1.2 g/kg HEP under heat stress. T4 = fed basal diet with 1.6 g/kg HEP under heat stress. For each broiler, five non-overlapping fields (upper, middle, lower, left, and right) were captured, and the number of positive cells per field was counted using ImageJ. The average number of positive cells per field across the five fields was calculated for each broiler, and the pen mean (six broilers per pen) was used as the experimental unit for statistical analysis. Post hoc multiple comparisons versus CON were performed using Dunnett's test based on EMMs (* $p < 0.05$, ** $p < 0.01$). Post hoc multiple comparisons versus HSG were performed using Dunnett's test based on EMMs ($^{\#}$ $p < 0.05$, $^{\#\#}$ $p < 0.01$). Values without any superscript symbol indicate no significant difference from either the CON or HSG ($p > 0.05$). Values are presented as estimated marginal means (EMMs) ± standard error (SE) based on a linear mixed model (LMM), with pen considered as a random effect. The pen was the experimental unit ($n = 6$ pens/treatment). There were 6 replicates (pens) per treatment, with 6 birds sampled per pen (36 birds per treatment).

3.6. Effects of HEP on mRNA Expression of Genes Related to Cell Proliferation, Apoptosis, and Autophagy in Immune Organs

In the thymus, heat stress significantly decreased *PCNA* mRNA expression by 51.8% and increased *caspase-3* mRNA expression by 127.3% compared with the CON ($p < 0.01$; Figure 6A,B). Compared with the HSG, *PCNA* mRNA expression increased by 127.7% and 118.8% in the T3 and T4 groups, respectively ($p < 0.01$), whereas *caspase-3* mRNA expression

decreased by 40.4%, 38.5%, and 64.3% in the T1, T3, and T4 groups, respectively ($p < 0.05$ or $p < 0.01$). In the spleen, heat stress significantly decreased *PCNA* mRNA expression by 31.7% and increased *caspase-3* mRNA expression by 110.1% compared with the CON ($p < 0.05$ or $p < 0.01$; Figure 6C,D). Compared with the HSG, *PCNA* mRNA expression increased by 74.6% and 87.3% in the T3 and T4 groups, respectively ($p < 0.01$), while *caspase-3* mRNA expression decreased by 68.4% in the T4 group ($p < 0.01$). In the bursa of Fabricius, no significant differences in *PCNA* mRNA expression were observed among the treatment groups ($p > 0.05$; Figure 6E). Compared with the HSG, *caspase-3* mRNA expression decreased by 33.7% in the T4 group ($p < 0.01$; Figure 6F).

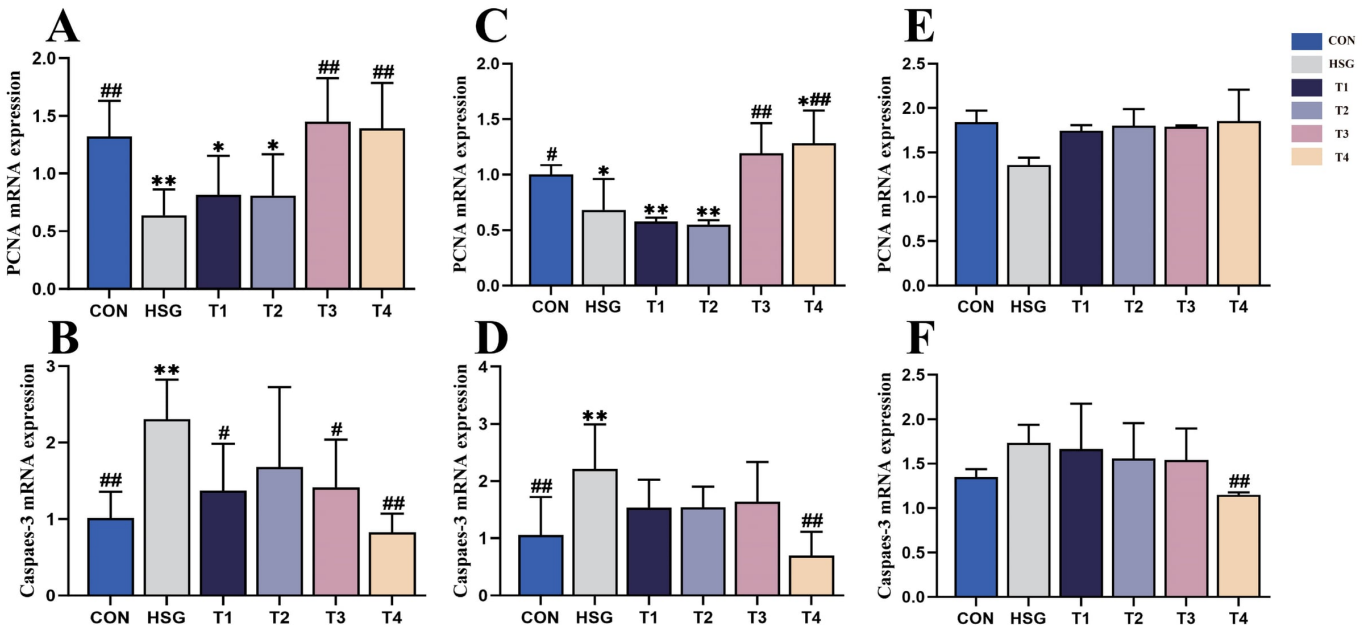

Figure 6. Effect of *Hericium erinaceus* polysaccharide-rich extract on the expression of cell proliferation- and apoptosis-related genes in immune organs of heat-stressed broilers. (**A**,**B**): thymus. (**C**,**D**): spleen. (**E**,**F**): bursa of Fabricius. (**A**,**C**,**E**): relative expression of *PCNA* mRNA. (**B**,**D**,**F**): relative expression of *Caspase-3* mRNA. CON = fed basal diet under thermoneutral conditions. HSG = fed basal diet under heat stress. T1 = fed basal diet with 0.4 g/kg HEP under heat stress. T2 = fed basal diet with 0.8 g/kg HEP under heat stress. T3 = fed basal diet with 1.2 g/kg HEP under heat stress. T4 = fed basal diet with 1.6 g/kg HEP under heat stress. *PCNA* = *proliferating cell nuclear antigen*. *Caspase-3* = *cysteinyl aspartate-specific proteinase-3*. Post hoc multiple comparisons versus CON were performed using Dunnett's test based on EMMs (* $p < 0.05$, ** $p < 0.01$). Post hoc multiple comparisons versus HSG were performed using Dunnett's test based on EMMs ($^{\#}$ $p < 0.05$, $^{\#\#}$ $p < 0.01$). Values without any superscript symbol indicate no significant difference from either the CON or HSG ($p > 0.05$). Values are presented as estimated marginal means (EMMs) ± standard error (SE) based on a linear mixed model (LMM), with pen considered as a random effect. The pen was the experimental unit ($n = 6$ pens/treatment). There were 6 replicates (pens) per treatment, with 6 birds sampled per pen (36 birds per treatment).

In the thymus, heat stress significantly increased *LC3B*, *BECN1*, and *ATG5* mRNA expression by 127.3%, 62.1%, and 229.5%, respectively, compared with the CON ($p < 0.01$; Figure 7A–C). Compared with the HSG, *LC3B* mRNA expression decreased by 40.4%, 38.5%, and 64.3% in the T1, T3, and T4 groups, respectively ($p < 0.05$ or $p < 0.01$). *BECN1* mRNA expression decreased by 34.9% in the T4 group ($p < 0.01$), while *ATG5* mRNA expression decreased by 65.2%, 44.4%, and 85.1% in the T2, T3, and T4 groups, respectively ($p < 0.05$ or $p < 0.01$). In the spleen, heat stress significantly increased *LC3B*, *BECN1*, and *ATG5* mRNA expression by 152.8%, 395.4%, and 103.3%, respectively, compared with the CON ($p < 0.01$;

Figure 7D–F). Compared with the HSG, *LC3B* mRNA expression decreased by 56.0% in the T4 group ($p < 0.01$), whereas *BECN1* mRNA expression decreased by 33.8%, 61.9%, 67.8%, and 66.9% in the T1, T2, T3, and T4 groups, respectively ($p < 0.05$ or $p < 0.01$). Additionally, *ATG5* mRNA expression decreased by 27.4% and 43.3% in the T2 and T4 groups, respectively ($p < 0.05$ or $p < 0.01$). In the bursa of Fabricius, heat stress significantly increased *LC3B*, *BECN1*, and *ATG5* mRNA expression by 63.8%, 147.1%, and 47.2%, respectively, compared with the CON ($p < 0.01$; Figure 7G–I). Compared with the HSG, *LC3B* mRNA expression decreased by 27.4%, 41.4%, and 47.6% in the T2, T3, and T4 groups, respectively ($p < 0.01$). Similarly, *BECN1* mRNA expression decreased by 27.2%, 33.1%, and 41.9%, respectively ($p < 0.05$ or $p < 0.01$), while *ATG5* mRNA expression decreased by 33.5%, 54.0%, 58.8%, and 64.5% in the T1, T2, T3, and T4 groups, respectively ($p < 0.01$).

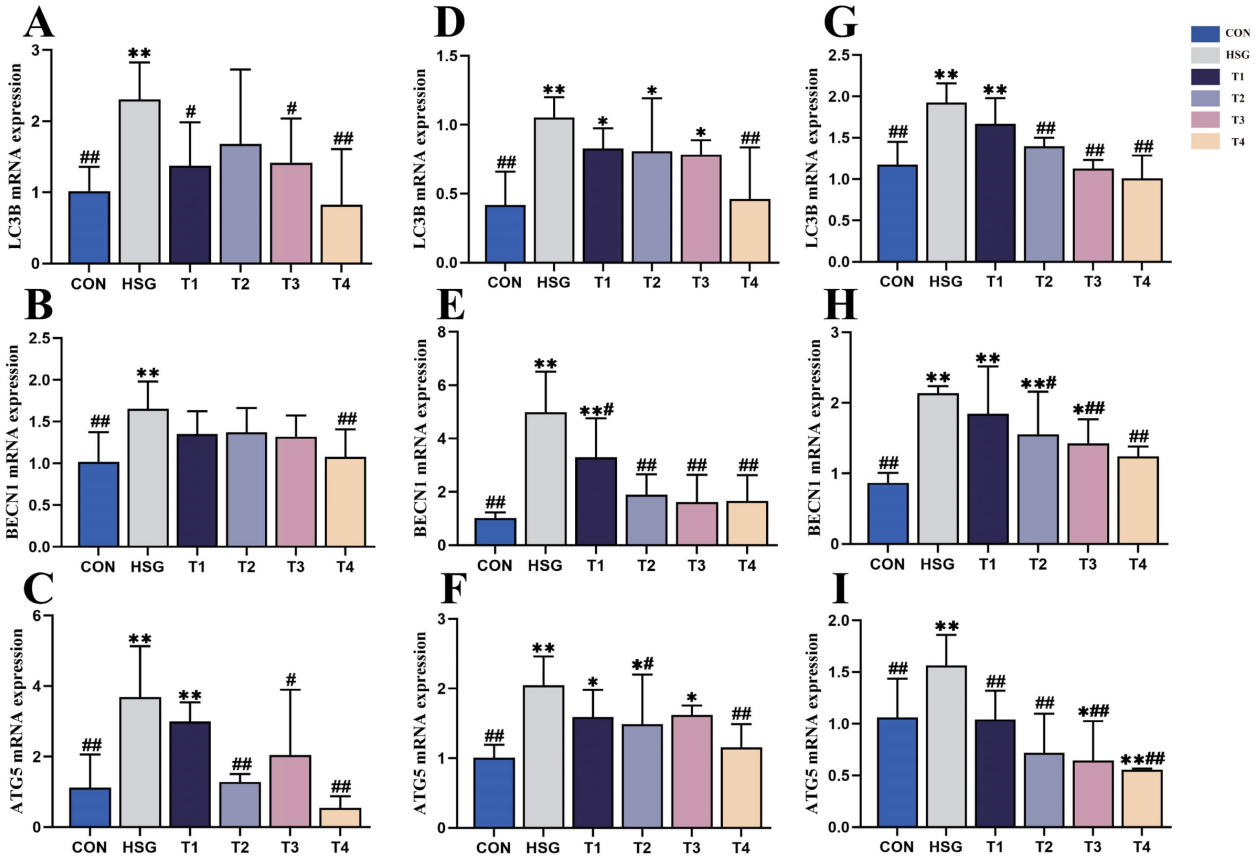

Figure 7. Effect of *Hericium erinaceus* polysaccharide-rich extract on the expression of autophagy-related genes in immune organs of heat-stressed broilers. (**A**–**C**): thymus. (**D**–**F**): spleen. (**G**–**I**): bursa of Fabricius. (**A**,**D**,**G**): relative expression of *LC3B* mRNA. (**B**,**E**,**H**): relative expression of *BECN1* mRNA. (**C**,**F**,**I**): relative expression of *ATG5* mRNA. CON = fed basal diet under thermoneutral conditions. HSG = fed basal diet under heat stress. T1 = fed basal diet with 0.4 g/kg HEP under heat stress. T2 = fed basal diet with 0.8 g/kg HEP under heat stress. T3 = fed basal diet with 1.2 g/kg HEP under heat stress. T4 = fed basal diet with 1.6 g/kg HEP under heat stress. *LC3B* = *microtubule-associated protein 1 light chain 3. BECN1* = *beclin 1. ATG5* = *autophagy-related 5*. Post hoc multiple comparisons versus CON were performed using Dunnett's test based on EMMs (* $p < 0.05$, ** $p < 0.01$). Post hoc multiple comparisons versus HSG were performed using Dunnett's test based on EMMs ($^{\#}$ $p < 0.05$, $^{\#\#}$ $p < 0.01$). Values without any superscript symbol indicate no significant difference from either the CON or HSG ($p > 0.05$). Values are presented as estimated marginal means (EMMs) ± standard error (SE) based on a linear mixed model (LMM), with pen considered as a random effect. The pen was the experimental unit ($n = 6$ pens/treatment). There were 6 replicates (pens) per treatment, with 6 birds sampled per pen (36 birds per treatment).

3.7. Effects of HEP on the Immunofluorescence Signals of PCNA, Caspase-3, and LC3B in Immune Organs

In the thymus, compared with the CON, the HSG showed a 14.7% decrease in PCNA AOD values and approximately 19.0% and 20.3% increases in caspase-3 and LC3B AOD values, respectively ($p < 0.01$; Figures 8G, 9G and 10G). Compared with the HSG, PCNA AOD values increased by 13.0%, 15.5%, and 16.3% in the T2, T3, and T4 groups, respectively ($p < 0.01$), whereas caspase-3 AOD values decreased by approximately 1.6%, 13.3%, and 15.4% in the T2, T3, and T4 groups, respectively ($p < 0.05$ or $p < 0.01$). LC3B AOD values decreased by 2.8%, 6.9%, and 13.2% in the T2, T3, and T4 groups, respectively ($p < 0.01$). In the spleen, compared with the CON, the HSG showed a 15.6% decrease in PCNA AOD values and approximately 10.8% and 20.1% increases in caspase-3 and LC3B AOD values, respectively ($p < 0.01$; Figures 8N, 9N and 10N). Compared with the HSG, PCNA AOD values increased by 6.6%, 11.3%, 13.4%, and 16.4% in the T1, T2, T3, and T4 groups, respectively ($p < 0.01$). Caspase-3 AOD values decreased by 9.6% and 18.6% in the T3 and T4 groups, respectively ($p < 0.01$), while LC3B AOD values decreased by approximately 1.6%, 1.6%, and 10.9% in the T2, T3, and T4 groups, respectively ($p < 0.05$ or $p < 0.01$). In the bursa of Fabricius, compared with the CON, the HSG showed a 47.3% decrease in PCNA AOD values and approximately 82.2% and 19.8% increases in caspase-3 and LC3B AOD values, respectively ($p < 0.01$; Figures 8U, 9U and 10U). Compared with the HSG, PCNA AOD values increased by 89.2%, 86.8%, 79.6%, and 57.1% in the T1, T2, T3, and T4 groups, respectively ($p < 0.01$). Caspase-3 AOD values decreased by approximately 2.7%, 12.5%, and 13.5% in the T2, T3, and T4 groups, respectively ($p < 0.01$), while LC3B AOD values decreased by 2.7%, 4.8%, and 16.7% in the T2, T3, and T4 groups, respectively ($p < 0.05$ or $p < 0.01$).

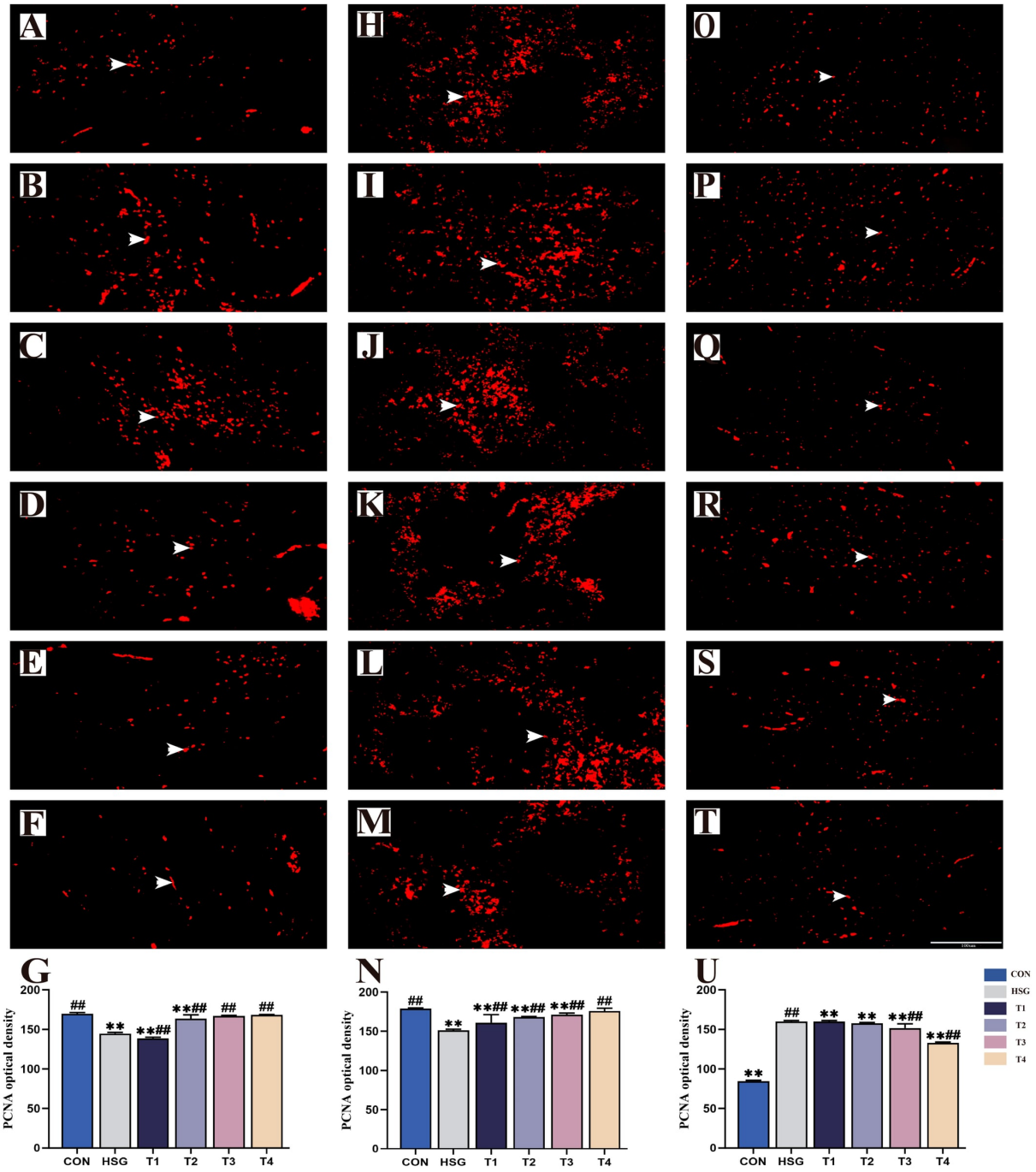

Figure 8. Effects of *Hericium erinaceus* polysaccharide-rich extract on PCNA immunofluorescence staining-positive cells in immune organs of heat-stressed broilers. (**A**,**H**,**O**): CON. (**B**,**I**,**P**): HSG. (**C**,**J**,**Q**): T1. (**D**,**K**,**R**): T2. (**E**,**L**,**S**): T3. (**F**,**M**,**T**): T4. (**A**–**F**): representative immunofluorescence image of PCNA in the thymus. (**H**–**M**): representative immunofluorescence image of PCNA in the spleen. (**O**–**T**): representative immunofluorescence image of PCNA in the bursa of Fabricius. (**G**): quantification of PCNA fluorescence optical density in the thymus. (**N**): quantification of PCNA fluorescence optical density in the spleen. (**U**): quantification of PCNA fluorescence optical density in the bursa of Fabricius. CON = fed basal diet under thermoneutral conditions. HSG = fed basal diet under heat stress. T1 = fed basal diet with 0.4 g/kg HEP under heat stress. T2 = fed basal diet with 0.8 g/kg HEP under heat stress. T3 = fed basal diet with 1.2 g/kg HEP under heat stress. T4 = fed basal diet with 1.6 g/kg HEP under heat stress. PCNA = proliferating cell nuclear antigen. Scale bar: 100 μm. Post hoc multiple comparisons versus CON were performed using Dunnett's test based on EMMs (** $p < 0.01$). Post hoc multiple comparisons versus HSG were performed using Dunnett's test based on EMMs ($^{\#\#}$ $p < 0.01$). Values without any superscript symbol indicate no significant

difference from either the CON or HSG ($p > 0.05$). Values are presented as estimated marginal means (EMMs) ± standard error (SE) based on a linear mixed model (LMM), with pen considered as a random effect. The pen was the experimental unit ($n = 6$ pens/treatment). There were 6 replicates (pens) per treatment, with 6 birds sampled per pen (36 birds per treatment).

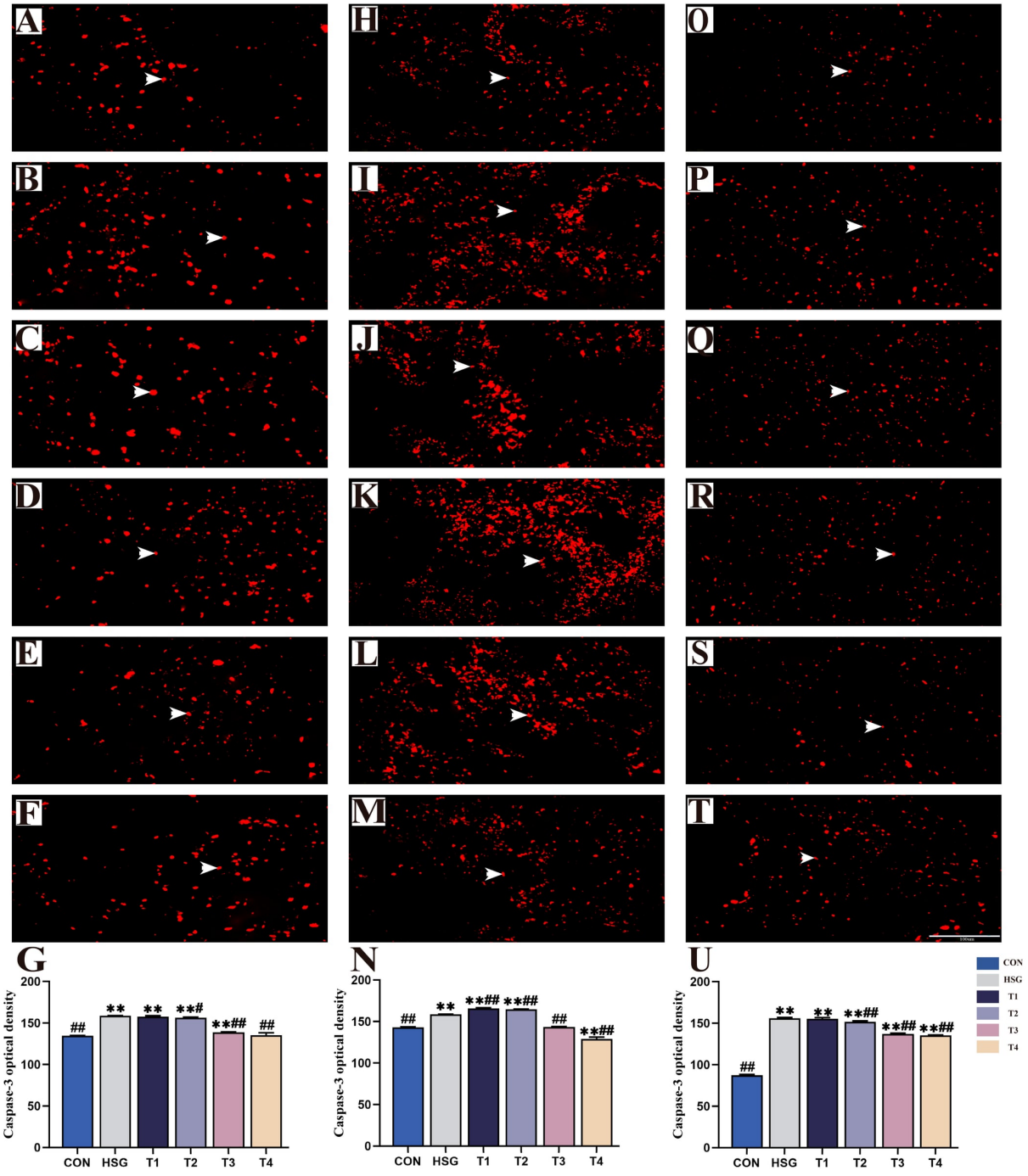

Figure 9. Effects of *Hericium erinaceus* polysaccharide-rich extract on caspase-3 immunofluorescence staining-positive cells in immune organs of heat-stressed broilers. (**A**,**H**,**O**): CON. (**B**,**I**,**P**): HSG. (**C**,**J**,**Q**): T1. (**D**,**K**,**R**): T2. (**E**,**L**,**S**): T3. (**F**,**M**,**T**): T4. (**A**–**F**): representative immunofluorescence image of caspase-3 in the thymus. (**H**–**M**): representative immunofluorescence image of caspase-3 in the spleen. (**O**–**T**): representative immunofluorescence image of caspase-3 in the bursa of Fabricius. (**G**): quantification of caspase-3 fluorescence optical density in the thymus. (**N**): quantification of caspase-3 fluorescence optical density in the spleen. (**U**): quantification of caspase-3 fluorescence optical density in the bursa of Fabricius. CON = fed basal diet under thermoneutral conditions. HSG = fed basal diet under heat stress. T1 = fed basal diet with 0.4 g/kg HEP under heat stress.

T2 = fed basal diet with 0.8 g/kg HEP under heat stress. T3 = fed basal diet with 1.2 g/kg HEP under heat stress. T4 = fed basal diet with 1.6 g/kg HEP under heat stress. Caspase-3 = cysteinyl aspartate-specific proteinase-3. Scale bar: 100 μm. Post hoc multiple comparisons versus CON were performed using Dunnett's test based on EMMs (** $p < 0.01$). Post hoc multiple comparisons versus HSG were performed using Dunnett's test based on EMMs ($^{\#}$ $p < 0.05$, $^{\#\#}$ $p < 0.01$). Values without any superscript symbol indicate no significant difference from either the CON or HSG ($p > 0.05$). Values are presented as estimated marginal means (EMMs) ± standard error (SE) based on a linear mixed model (LMM), with pen considered as a random effect. The pen was the experimental unit (n = 6 pens/treatment). There were 6 replicates (pens) per treatment, with 6 birds sampled per pen (36 birds per treatment).

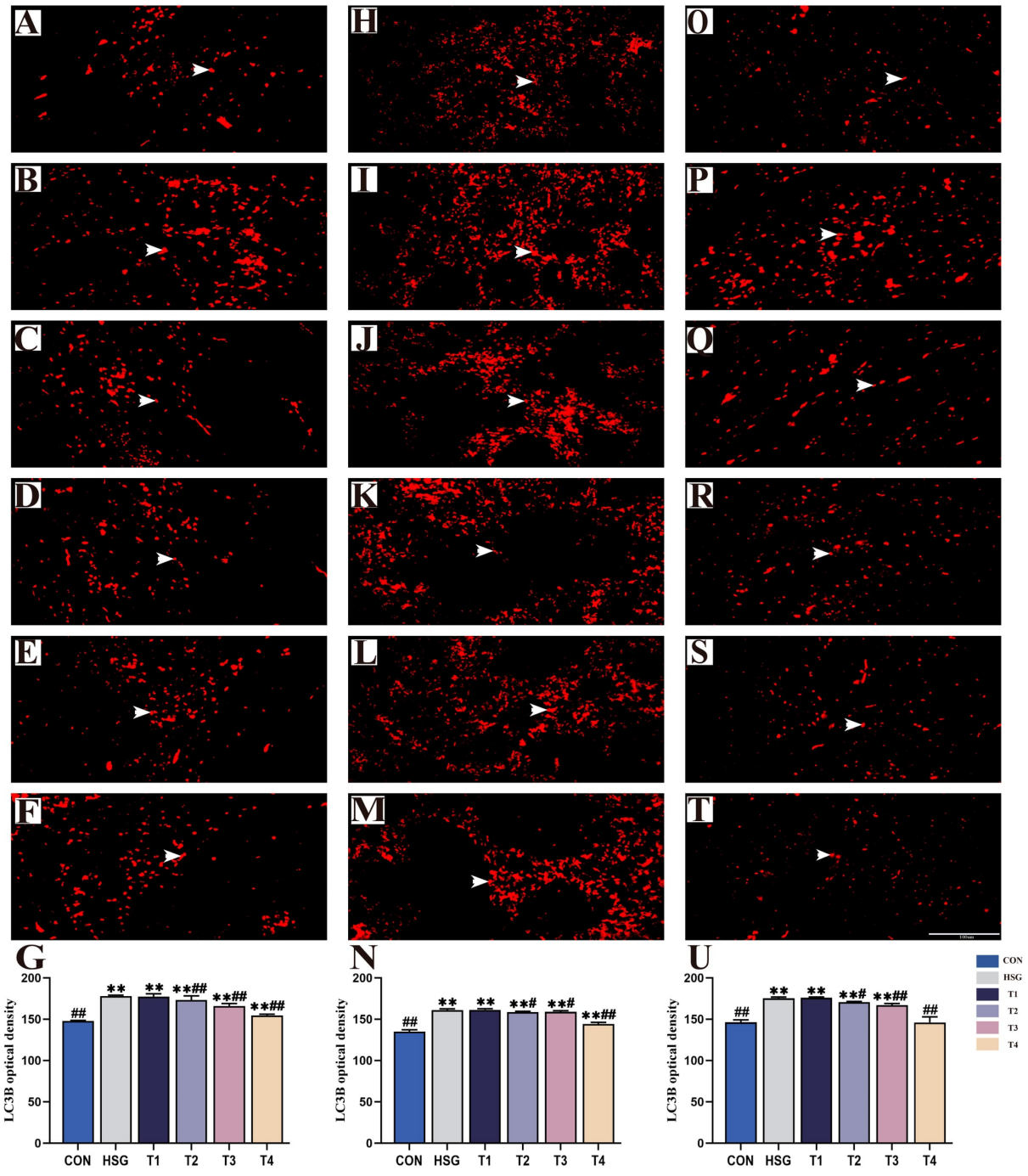

Figure 10. Effects of *Hericium erinaceus* polysaccharide-rich extract on LC3B immunofluorescence staining-positive cells in immune organs of heat-stressed broilers. (**A**,**H**,**O**): CON. (**B**,**I**,**P**): HSG. (**C**,**J**,**Q**): T1. (**D**,**K**,**R**): T2. (**E**,**L**,**S**): T3. (**F**,**M**,**T**): T4. (**A**–**F**): representative immunofluorescence image

of LC3B in the thymus. (**H**–**M**): representative immunofluorescence image of LC3B in the spleen. (**O**–**T**): representative immunofluorescence image of LC3B in the bursa of Fabricius. (**G**): quantification of LC3B fluorescence optical density in the thymus. (**N**): quantification of LC3B fluorescence optical density in the spleen. (**U**): quantification of LC3B fluorescence optical density in the bursa of Fabricius. CON = fed basal diet under thermoneutral conditions. HSG = fed basal diet under heat stress. T1 = fed basal diet with 0.4 g/kg HEP under heat stress. T2 = fed basal diet with 0.8 g/kg HEP under heat stress. T3 = fed basal diet with 1.2 g/kg HEP under heat stress. T4 = fed basal diet with 1.6 g/kg HEP under heat stress. LC3B = microtubule-associated protein 1 light chain 3. Scale bar: 100 μm. Post hoc multiple comparisons versus CON were performed using Dunnett's test based on EMMs (** $p < 0.01$). Post hoc multiple comparisons versus HSG were performed using Dunnett's test based on EMMs ($^{\#}$ $p < 0.05$, $^{\#\#}$ $p < 0.01$). Values without any superscript symbol indicate no significant difference from either the CON or HSG ($p > 0.05$). Values are presented as estimated marginal means (EMMs) ± standard error (SE) based on a linear mixed model (LMM), with pen considered as a random effect. The pen was the experimental unit ($n = 6$ pens/treatment). There were 6 replicates (pens) per treatment, with 6 birds sampled per pen (36 birds per treatment).

4. Discussion

The present study was designed to evaluate whether dietary HEP supplementation could alleviate heat stress-induced impairment of immune function in broilers and to examine the associated changes in immune cell proliferation, apoptosis, and autophagy. It was hypothesized that HEP would improve growth performance and immune organ antioxidant status in heat-stressed broilers, and that these effects would be accompanied by modulation of PCNA-, caspase-3-, and autophagy-related gene expression. The Discussion section continued below interprets the observed effects in relation to these objectives, while distinguishing between findings directly supported by the data obtained in this study and mechanisms proposed on the basis of the existing literature.

4.1. HEP Improves the Growth Performance of Heat-Stressed Broilers

The present study demonstrated that dietary HEP supplementation improved ADG, ADFI, and F/G in heat-stressed broilers, with the largest responses observed in the T3 and T4 groups, indicating that HEP can mitigate the adverse effects of heat stress on broiler growth performance. In addition, the growth-promoting effect of HEP showed a trend consistent with a dose-dependent response, with the T3 and T4 groups numerically exceeding the T1 and T2 groups. One possible explanation is that higher HEP doses supply more fermentable monosaccharides; however, this remains speculative because monosaccharide availability at the intestinal level was not measured in this study. Environmental temperature and humidity control remain the primary measures for reducing heat stress, but precise control can be costly in intensive production systems. Nutritional intervention therefore provides a complementary strategy [29]. Fungal polysaccharides such as Ganoderma lucidum polysaccharides and lentinan have been shown to promote animal growth performance and enhance immune function. Li et al. found that dietary lentinan improved production performance, meat quality, and immune function in broilers [30]. Lv et al. found that dietary supplementation with Astragalus polysaccharides improved intestinal microbiota, thereby improving production performance and egg quality in Chongren hens [31]. These studies collectively indicate that fungal polysaccharides exert notable beneficial effects on animal growth and development. HEP is a candidate feed additive because it combines antioxidant and immunomodulatory activities with established production methods [32,33]. Therefore, HEP has promising application prospects in alleviating heat stress and improving growth performance in broilers.

4.2. HEP Enhances the Immune and Antioxidant Functions of Heat-Stressed Broilers

Heat stress can disrupt immune homeostasis by altering pro-inflammatory and anti-inflammatory cytokine signaling and impairing immune organ development [34,35]. In the present study, dietary HEP supplementation modulated the cytokine profiles in heat-stressed broilers, reducing the pro-inflammatory cytokines IL-1β and TNF-α, while also regulating IL-4 levels, and improved the morphology of immune organs. The alleviating effects varied across different immune organs, with the most pronounced responses generally observed at moderate-to-high supplementation levels (T3 and T4). These findings suggest that HEP can help regulate immune homeostasis under heat stress conditions. The observed effects may be associated with the chemical features of HEP, although the present study did not directly test structure–activity relationships. Previous studies have reported that the immunomodulatory activity of *Hericium erinaceus* polysaccharide has been attributed to its β-1,3 and β-1,6 glycosidic linkages [14,36]. *Hericium erinaceus* polysaccharide has been reported to activate signaling pathways such as TLR4/MyD88/NF-κB, MAPK, and PI3K/Akt, leading to the phosphorylation of IκB-α, p38, JNK, ERK, and PKB/Akt and enhanced expression of cytokines including TNF-α, IL-6, and IFN-γ [14]. Yu et al. showed that selenium-modified *Hericium erinaceus* polysaccharide enhanced the expression of CD86 and MHC-II in dendritic cells (DCs) and increased the levels of IL-12 and TNF-α, and they confirmed that this process resulted from enhanced DC immune activity via activation of the TLR4/MyD88/NF-κB signaling pathway [37]. Ren et al. showed that low-molecular-weight *Hericium erinaceus* polysaccharide reduced the secretion of inflammatory cytokines induced by lipopolysaccharide (LPS) or dextran sulfate sodium (DSS) and inhibited NLRP3 inflammasome activation and the phosphorylation of NF-κB, AKT, and MAPK, thereby improving immune function in mice [38]. In addition, oral administration of the polysaccharide from *Hericium erinaceus* mycelium ameliorated ulcerative colitis (UC)-induced mitochondrial morphological abnormalities in rat intestinal epithelial cells, and mitochondrial swelling and membrane rupture were no longer observed [39]. Collectively, these findings indicate that HEP plays an important regulatory role in alleviating inflammation-induced oxidative stress and mitochondrial dysfunction. Based on these literature reports, it is plausible that glucose and mannose in HEP may activate TLR-mediated, MyD88-dependent signaling pathways, thereby activating NF-κB; inducing the expression of cytokines such as TNF-α, IL-6, and IFN-γ; and ultimately enhancing cellular immune function; however, this mechanism was not examined in the present study and remains to be verified.

Compared with the heat stress group, appropriate HEP supplementation significantly decreased MDA levels, enhanced T-SOD activity, and increased GSH-Px content and T-AOC in immune organs, with the most pronounced effect observed in the T4 group. This suggests that broilers under heat stress may require a relatively high dose of HEP to effectively restore oxidative balance. Although this speculation still requires further mechanistic verification, higher HEP doses contain more glucose and mannose, which could potentially support cellular metabolism; however, this possibility was not directly assessed in the present study. Studies have confirmed that heat stress can impair the antioxidant defense systems of animals, leading to reactive oxygen species accumulation and lipid peroxidation, whereas plant polysaccharides can enhance the endogenous antioxidant capacity of animals to improve oxidative balance under heat stress [11,40]. Previous studies have shown that *Ulva* polysaccharide (SDP) can improve the antioxidant capacity of the spleen and reduce MDA levels in heat-stressed broilers by enhancing the Nrf2 signaling pathway, while inhibiting the NF-κB p65 signaling pathway to alleviate splenic inflammation [41]. *Cyclocarya paliurus* polysaccharide (CPP) can activate stress-induced genes (sod-3, sod-5, ctl-1, ctl-2, etc.) through skn-1 and hsf-1, thereby enhancing the resistance of *Cyclocarya paliurus* to heat stress and oxidative stress [42]. Han et al. found that in immunosuppressed mice, 320 mg/kg

Hericium erinaceus polysaccharide significantly enhanced T-SOD activity, increased T-AOC and GSH-Px content, and improved the microstructures of immune organs (thymus and spleen) [15]. Tu et al. showed that *Hericium erinaceus* polysaccharide can directly scavenge 1,1-diphenyl-2-picrylhydrazyl (DPPH), hydroxyl radicals, superoxide anions, and 2,2′-azino-bis (3-ethylbenzothiazoline-6-sulfonic acid) (ABTS) radicals, and that its ABTS radical scavenging capacity increased with concentration [43]. Qiu et al. also found that *Hericium erinaceus* polysaccharide alleviated intestinal oxidative damage in heat-stressed ducks by reducing lipid peroxidation and enhancing antioxidant defense [44]. In addition, *Hericium erinaceus* polysaccharide can inhibit free radical generation, alleviate mitochondrial dysfunction, and protect mitochondrial integrity and function, suggesting that the antioxidant function of *Hericium erinaceus* polysaccharide is closely related to mitochondrial integrity [45]. Although mitochondrial integrity was not assessed in the present study, these literature findings raise the possibility that mitochondrial protection may contribute to the antioxidant effects of HEP. Previous studies have suggested that the antioxidant activity of HEP may be related to its high content of glucose, mannose, and galactose, with mannose and galactose reported to enhance free radical scavenging and reducing capacity and synergistically activate macrophages, thereby modulating intracellular endogenous antioxidant enzyme activity [46]. These mechanisms, however, were not directly tested here.

4.3. HEP Regulates Immune Cell Proliferation, Apoptosis, and Autophagy in Heat-Stressed Broilers

The dynamic balance between cell proliferation and apoptosis is the basis for the normal development of immune organs, and excessive imbalance can disrupt immune homeostasis [47,48]. Proliferating cell nuclear antigen (PCNA) is a nuclear protein specifically expressed in the late G1 and S phases of the cell cycle. It regulates DNA replication and repair by interacting with cell cycle regulators and is a key marker of the proliferative status of immune cells [49]. Studies have shown that the immunologically active center of oligosaccharide fragments from Astragalus polysaccharides lies in the glycan region with a degree of polymerization of 9–19; these fragments enhance tyrosine phosphorylation of insulin receptor substrate 1 by activating the PI3K/Akt signaling pathway, thereby dose-dependently promoting cell proliferation and upregulating PCNA [50]. The arabinogalactan structure rich in arabinose and galactose in *Lycium barbarum* polysaccharides is a key structural element recognized and activated by immune cells [51]. Among the monosaccharides in these two polysaccharides, glucose is the most abundant. In the present study, dietary HEP supplementation promoted PCNA expression in immune cells, decreased caspase-3 expression, and improved the histological parameters of immune organs. Moreover, compared with the T1 group, the T3 and T4 groups showed more PCNA-positive cells in immune organs, and the T4 group had the fewest apoptotic cells. These findings indicate that HEP maintains proliferation–apoptosis homeostasis in immune cells under heat stress by promoting proliferation and inhibiting excessive apoptosis, which may be mainly related to its glucose-rich nature. Nevertheless, explaining its immunomodulatory activity solely on the basis of glycosidic bond types and monosaccharide composition has limitations, and the underlying mechanisms require further investigation. Liu et al. purified homogeneous polysaccharides CASP-0 and CASP-3 from *Stropharia rugosoannulata*, in which glucose accounted for up to 83.76% and 89.72% (molar percentage) of the monosaccharide composition, respectively [52]. Both polysaccharides significantly inhibited the proliferation of colon cancer HT-29 cells in a dose- and time-dependent manner and induced apoptosis by upregulating caspase-3 and Bax expression and downregulating Bcl-2 expression, suggesting that their apoptosis-inducing effect is closely related to the monosaccharide ratio. In addition, in immunosuppressed mouse models, supplementation with 320 mg/kg *Hericium erinaceus* polysaccharide significantly increased *PCNA* mRNA expression and

decreased *caspase-3* mRNA expression in the thymus and spleen, and it improved immune organ microstructure [15]. In aged laying hens, *Hericium erinaceus* polysaccharide similarly promoted the expression of *PCNA* and *Ki-67* in uterine tissues and downregulated the mRNA levels of *caspase-3* and *caspase-9* [18]. These studies indicate that *Hericium erinaceus* polysaccharide does not simply promote proliferation or inhibit apoptosis but regulates both processes, maintaining immune cell renewal and survival at appropriate levels [53].

Autophagy is a conserved degradation pathway that maintains cellular homeostasis under conditions such as heat stress and oxidative damage [54]. Heat stress can induce the expression of autophagy-related genes in immune organs [55]. In the present study, heat stress significantly upregulated the mRNA expression of autophagy-related genes (*LC3B*, *BECN1*, and *ATG5*) in immune organs, whereas HEP supplementation decreased the expression levels of these genes in all examined tissues, with the most pronounced reduction observed in the T4 group. The reduction in autophagy-related gene expression may be related to the β-glucan-rich structure of *Hericium erinaceus* polysaccharide, as β-1,3 and β-1,6 glycosidic linkages can be recognized by immune cell surface receptors [56,57]. However, receptor binding and downstream signaling were not directly examined in this study, and this interpretation therefore remains speculative. Similar β-1,3 backbone structures in lentinan β-glucan can promote autophagic flux through the AMPK/mTOR signaling pathway, accelerating the clearance of damaged components [58]. These studies indicate that the structural characteristics of β-glucan, including backbone linkage type, degree of branching, and molecular weight, are key factors determining its autophagy-regulatory activity. In neuroprotective research, an ethanol extract of *Hericium erinaceus* mycelia has been shown to prevent the accumulation and spread of α-synuclein and β-amyloid and to regulate LC3-II expression by activating the SIRT-1/ERK-1/2-mediated autophagy signaling pathway [59]. In addition, polysaccharide components present in microbial cell-free supernatants of *Hericium erinaceus* and *Ganoderma lucidum* can upregulate PCNA, SOD1, SQSTM/p62, and beclin 1 through AhR activation, thereby promoting hippocampal neuronal proliferation and modulating autophagy [53]. These studies suggest that the β-glucan structure of HEP may regulate autophagy intensity through similar receptor recognition and signal transduction mechanisms. The anti-autophagic effect of the T4 group was superior to those of the low-dose groups, suggesting that heat-stressed broilers require a relatively high dose of HEP to effectively alleviate oxidative stress and downregulate autophagy-related gene expression. The HEP-induced reduction in autophagy-related gene expression may not reflect direct inhibition of autophagy initiation, but rather reduced cellular demand for stress-induced autophagic protection secondary to improved antioxidant status. This interpretation is indirect, because autophagic flux, lysosomal function, and upstream regulatory kinases were not measured; therefore, the structure–activity relationship underlying the autophagy-regulatory activity of HEP requires further investigation.

5. Conclusions

In conclusion, dietary HEP supplementation improved growth performance, antioxidant status, and cytokine profiles and was associated with improved histological characteristics of immune organs in heat-stressed broilers. Furthermore, HEP supplementation altered the expression of genes and proteins associated with cell proliferation (PCNA), apoptosis (caspase-3), and autophagy (LC3B, BECN1, and ATG5), with increased PCNA-related signals and generally reduced caspase-3- and autophagy-related marker levels in selected immune organs. These findings indicate that HEP has potential as a functional feed additive to support immune health and alleviate the adverse effects of heat stress in poultry production. Dietary supplementation with 1.2–1.6 g/kg HEP may be a promising nutritional

strategy for heat-stressed broilers. Further studies are needed to evaluate its long-term effects and cost-effectiveness under large-scale commercial production conditions.

Supplementary Materials: The following supporting information can be downloaded at: https://www.mdpi.com/article/10.3390/antiox15121558/s1, Table S1: Composition and nutrient levels of basal diets (air-dry basis)%; Table S2: Real-time fluorescence quantitative primer sequences.

Author Contributions: C.Z. (Chaohui Zhang): Investigation, Methodology, Experiment design, Data analysis, Writing—original draft. Y.Z.: Validation, Sample collection, Supervision. J.W.: Sample collection, Supervision. C.W., M.R., W.W., C.Z. (Chunfang Zhao), J.T. and W.C.: Validation, Supervision. S.L.: Writing—review and editing. E.J.: Formal analysis, Supervision, Writing—review and editing. All authors have read and agreed to the published version of the manuscript.

Funding: This work was supported by the National Natural Science Foundation of China (32172816), the Natural Science Key Foundation of Anhui Education Department (2022AH040032), the Veterinary Science Peak Discipline Project of Anhui Science and Technology University (XK-XJGF002), and the Food and Nutrition Peak Discipline Project of Anhui Science and Technology University (XK-XJGF003).

Institutional Review Board Statement: The experimental protocol and sample collection were carried out in accordance with the regulations on the Administration of Laboratory Animals promulgated by the National Science and Technology Commission of the People's Republic of China. And the experiment was approved by the Committee of the College of Animal Science, Anhui Science and Technology University, Chuzhou, China (approval no. 2024217; approval date: 17 February 2024).

Informed Consent Statement: Not applicable.

Data Availability Statement: The original contributions presented in this study are included in the article/Supplementary Material. Further inquiries can be directed to the corresponding author.

Acknowledgments: The graphical abstract used the elements in BioGDP [27].

Conflicts of Interest: The authors declare no conflicts of interest.

Abbreviations

The following abbreviations are used in this manuscript:

HEP	*Hericium erinaceus* polysaccharide-rich extract
ADG	Average daily gain
ADFI	Average daily feed intake
F/G	Feed-to-gain ratio
IL-1β	Interleukin-1β
IL-4	Interleukin-4
TNF-α	Tumor necrosis factor-α
T-SOD	Total superoxide dismutase
GSH-Px	Glutathione peroxidase
T-AOC	Total antioxidant capacity
MDA	Malondialdehyde
PCNA	Proliferating cell nuclear antigen
Caspase-3	Cysteinyl aspartate-specific proteinase-3
LC3B	Microtubule-associated protein 1 light chain 3 beta
BECN1	Beclin 1
ATG5	Autophagy-related 5
BD	Basal diet
CO	Cortex
ME	Medulla
SN	Splenic nodule
LN	Follicular nodule

References

1. Oluwagbenga, E.M.; Fraley, G.S. Heat stress and poultry production: A comprehensive review. *Poult. Sci.* **2023**, *102*, 103141. [CrossRef] [PubMed]
2. Perederiy, D.B. The influence of heat stress on the antioxidant protection glutathione link and the content of lipid peroxidation products in chicken liver. *Anim. Biol.* **2023**, *25*, 51–57. [CrossRef]
3. Vandana, G.D.; Sejian, V.; Lees, A.M.; Pragna, P.; Silpa, M.V.; Maloney, S.K. Heat stress and poultry production: Impact and amelioration. *Int. J. Biometeorol.* **2021**, *65*, 163–179. [CrossRef] [PubMed]
4. Son, J.; Kim, H.J.; Hong, E.C.; Kang, H.K. Effects of Stocking Density on Growth Performance, Antioxidant Status, and Meat Quality of Finisher Broiler Chickens under High Temperature. *Antioxidants* **2022**, *11*, 871. [CrossRef] [PubMed]
5. Goel, A.; Ncho, C.M.; Gupta, V.; Choi, Y.H. Embryonic modulation through thermal manipulation and in ovo feeding to develop heat tolerance in chickens. *Anim. Nutr.* **2023**, *13*, 150–159. [CrossRef] [PubMed]
6. Rezar, V.; Pal, M.P.; Leskovec, J.; Levart, A.; Salobir, J.; Lavrenčič, A.; Vrecl, M.; Pirman, T. Combined Effects of Cyclic Heat Stress, Dietary Induced Oxidative Stress and Different Levels of Antioxidant on Gut Fermentation Activity and Mucosal Morphology in Broiler Chickens. *Agriculture* **2024**, *14*, 64. [CrossRef]
7. Uyanga, V.A.; Zhao, J.; Wang, X.; Jiao, H.; Onagbesan, O.M.; Lin, H. Dietary L-citrulline modulates the growth performance, amino acid profile, and the growth hormone/insulin-like growth factor axis in broilers exposed to high temperature. *Front. Physiol.* **2022**, *13*, 937443. [CrossRef] [PubMed]
8. Bai, S.; He, C.; Zhang, K.; Ding, X.; Zeng, Q.; Wang, J.; Peng, H.; Bai, J.; Lü, H.; Xuan, Y.; et al. Effects of dietary inclusion of Radix Bupleuri and Radix Astragali extracts on the performance, intestinal inflammatory cytokines expression, and hepatic antioxidant capacity in broilers exposed to high temperature. *Anim. Feed Sci. Technol.* **2019**, *259*, 114288. [CrossRef]
9. Zhou, H.J.; Wubuli, A.; Wu, Y.Y.; Lü, Z.; Li, J.Y. Research progress of polysaccharide structure-activity relationship. *Food Sci. Hum. Wellness* **2026**, *15*, 9250485. [CrossRef]
10. Hosseini-Vashan, S.J.; Piray, A.H. Effect of dietary saffron (Crocus sativus) petal extract on growth performance, blood biochemical indices, antioxidant balance, and immune responses of broiler chickens reared under heat stress conditions. *Ital. J. Anim. Sci.* **2021**, *20*, 1338–1347. [CrossRef]
11. Liu, W.C.; Liu, H.M.; Wang, Y.Y.; Zhao, Z.X.; Balasubramanian, B.; Jha, R. Effects of Enteromorpha prolifera polysaccharides on growth performance, intestinal barrier function and cecal microbiota in yellow-feathered broilers under heat stress. *J. Anim. Sci. Biotechnol.* **2023**, *14*, 132. [CrossRef] [PubMed]
12. He, X.; Wang, X.; Fang, J.; Chang, Y.S.; Ning, N.; Guo, H.; Huang, L.; Huang, X.; Zhao, Z. Structures, biological activities, and industrial applications of the polysaccharides from Hericium erinaceus (Lion's Mane) mushroom: A review. *Int. J. Biol. Macromol.* **2017**, *97*, 228–237. [CrossRef] [PubMed]
13. Kostanda, E.; Musa, S.; Pereman, I. Unveiling the Chemical Composition and Biofunctionality of Hericium spp. Fungi: A Comprehensive Overview. *Int. J. Mol. Sci.* **2024**, *25*, 5949. [CrossRef] [PubMed]
14. Niu, B.; Zhang, L.; Chen, B.; Liu, X.; Yang, F.; Ren, Y.; Xiang, H.; Wang, P.; Li, J. Extraction, purification, structural characteristics, biological activities, modifications, and applications from Hericium erinaceus polysaccharides: A review. *Int. J. Biol. Macromol.* **2024**, 138932. [CrossRef] [PubMed]
15. Han, Y.; Huang, J.; Zhao, C.; Zhang, F.; Gu, Y.; Wang, C.; Jin, E. Hericium erinaceus polysaccharide improves the microstructure, immune function, proliferation and reduces apoptosis of thymus and spleen tissue cells of immunosuppressed mice. *Biosci. Biotechnol. Biochem.* **2023**, *87*, 279–289. [CrossRef] [PubMed]
16. Li, J.; Mo, J.; Hu, S.; Dong, X.; Li, J.; Yang, L.C.; Wu, Y. Effects of Hericium erinaceus polysaccharide in porcine IPEC-J2 intestinal epithelial cells against apoptosis induced by oxidative stress. *Comp. Biochem Physiol. C Toxicol. Pharmacol.* **2024**, *280*, 109902. [CrossRef] [PubMed]
17. Zheng, L.; Wu, Y.; Liao, J.; Cai, D.; Zhang, Y.; Zhu, E.; Zhou, W.; Wu, B.; Huang, Y. Effect of hericium polysaccharide on partial cytokines and hormones in muscovy ducks infected with muscovy duck reovirus. *Chin. Vet. Sci.* **2017**, *47*, 249–256.
18. Wu, L.; Hu, Z.; Lv, Y.; Ge, C.; Luo, X.; Zhan, S.; Huang, W.; Shen, X.; Yu, D.; Liu, B. Hericium erinaceus polysaccharides improve eggshell quality by improving uterine health and modulating uterine microbiota in aged hens. *Anim. Nutr.* **2025**, *22*, 72–87. [CrossRef] [PubMed]
19. Zhang, N.; Tang, Z.; Zhang, J.; Li, X.; Yang, Z.; Yang, C.; Zhang, Z.; Huang, Z. Comparative transcriptome analysis reveals the genetic basis underlying the biosynthesis of polysaccharides in Hericium erinaceus. *Bot. Stud.* **2019**, *60*, 15. [CrossRef] [PubMed]
20. Chen, S.; Ling, B.; Liu, X.; Liu, L.; Feng, J.; Zhang, J.; Yang, Y.; Wu, D.; Guo, Q.; Liu, Y. Structural characterization of β-glucan in Hericium erinaceus pretreated by steam explosion and its effects on human gut microbiota in vitro. *Food Chem.* **2025**, *482*, 144156. [CrossRef] [PubMed]
21. Zhuang, H.N.; Dong, H.Y.; Zhang, X.W.; Feng, T. Antioxidant Activities and Prebiotic Activities of Water-Soluble, Alkali-Soluble Polysaccharides Extracted from the Fruiting Bodies of the Fungus Hericium erinaceus. *Polymers* **2023**, *15*, 4165. [CrossRef] [PubMed]

22. Min, L.; Huijuan, J.; Jianjun, Z.; Gen, C.; Meng, Z.; Zheng, G.; Shangshang, L.; Zhenzhen, R.; Long, H.; Yu, L.; et al. Optimization of Mycelia Selenium Polysaccharide Extraction from Agrocybe cylindracea SL-02 and Assessment of their Antioxidant and Anti-Ageing Activities. *PLoS ONE* **2016**, *11*, e0160799. [CrossRef] [PubMed]
23. *GB/T 5916-2008*; Formula Feeds for Laying Hens and Broiler Chickens. Standards Press of China: Beijing, China, 2008.
24. Jiang, H.; Huang, L.; Wu, B.; Li, J.; Wu, Y.; Huang, Y. Effects of Hericium Polysaccharide Powder on Mortality Rate and Intestinal Morphology of Muscovy Ducks Infected with Muscovy Duck Reovirus. *China Poult.* **2015**, *37*, 22–26.
25. Wu, L.; Lv, Y.; Ge, C.; Luo, X.; Hu, Z.; Huang, W.; Zhan, S.; Shen, X.; Yu, D.; Liu, B. Polysaccharide from Hericium erinaceus improved laying performance of aged hens by promoting yolk precursor synthesis and follicle development via liver-blood-ovary axis. *Poult. Sci.* **2024**, *103*, 103810. [CrossRef] [PubMed]
26. Abu-Dieyeh, Z.H.M. Effect of Chronic Heat Stress and Long-Term Feed Restriction on Broiler Performance. *Int. J. Poult. Sci.* **2006**, *5*, 185–190. [CrossRef]
27. Jiang, S.; Li, H.; Zhang, L.; Mu, W.; Zhang, Y.; Chen, T.; Wu, J.; Tang, H.; Zheng, S.; Liu, Y.; et al. Generic Diagramming Platform (GDP): A comprehensive database of high-quality biomedical graphics. *Nucleic Acids Res.* **2025**, *53*, D1670–D1676. [CrossRef]
28. Lugata, J.K.; Ndunguru, S.F.; Reda, G.K.; Ozsváth, X.E.; Angyal, E.; Czeglédi, L.; Gulyás, G.; Knop, R.; Oláh, J.; Mészár, Z.; et al. Methionine sources and genotype affect embryonic intestinal development, antioxidants, tight junctions, and growth-related gene expression in chickens. *Anim. Nutr. (Zhongguo Xu Mu Shou Yi Xue Hui)* **2023**, *16*, 218–230. [CrossRef] [PubMed]
29. Oni, A.I.; Adeleye, O.O.; Adebowale, T.; Oke, O.E. The role of phytogenic feed additives in stress mitigation in broiler chickens. *J. Anim. Physiol. Anim. Nutr.* **2023**, *108*, 81–98. [CrossRef] [PubMed]
30. Li, W.; Ai, Y. Effects of dietary lentinan on production performance, meat quality and immune function of broilers. *China Feed* **2022**, *10*, 40–43.
31. Lv, H.W.; Tang, Y.Q.; Zhang, H.H.; Li, S.M.; Fan, Z.Y. Astragalus polysaccharide supplementation improves production performance, egg quality, serum biochemical index and gut microbiota in Chongren hens. *Anim. Sci. J.* **2021**, *92*, e13550. [CrossRef] [PubMed]
32. Almjalawi, B.S.A.; Chechan, R.A.; Alhesnawi, A.S.M. Some Applications of Hericium erinaceus Mushrooms: A Review. *South Asian Res. J. Agric. Fish.* **2024**, *6*, 92–100. [CrossRef]
33. Gong, M.; Zhang, H.; Wu, D.; Zhang, Z.; Zhang, J.; Bao, D.; Yang, Y. Key metabolism pathways and regulatory mechanisms of high polysaccharide yielding in Hericium erinaceus. *BMC Genom.* **2021**, *22*, 160. [CrossRef] [PubMed]
34. Ding, K.N.; Lu, M.H.; Guo, Y.N.; Liang, S.S.; Mou, R.W.; He, Y.M.; Tang, L.P. Resveratrol relieves chronic heat stress-induced liver oxidative damage in broilers by activating the Nrf2-Keap1 signaling pathway. *Ecotoxicol. Environ. Saf.* **2023**, *249*, 114411. [CrossRef] [PubMed]
35. Wang, X.; Xi, J.; Chen, P.; Chen, Y.; Chen, K.; Zheng, W.; Zhao, Y. HSP104 and HSP20-L Are Required by Aspergillus nidulans in Response to Attack by Fungivorous Springtail Sinella curviseta. *Environ. Microbiol. Rep.* **2025**, *17*, e70147. [CrossRef] [PubMed]
36. Wu, L.; Hu, Z.; Lv, Y.; Ge, C.; Luo, X.; Zhan, S.; Huang, W.C.; Shen, X.; Yu, D.; Liu, B. Hericium erinaceus polysaccharides ameliorate nonalcoholic fatty liver disease via gut microbiota and tryptophan metabolism regulation in an aged laying hen model. *Int. J. Biol. Macromol.* **2024**, *273*, 132735. [CrossRef] [PubMed]
37. Yu, R.; Sun, M.; Meng, Z.; Zhao, J.; Qin, T.; Ren, Z. Immunomodulatory effects of polysaccharides enzymatic hydrolysis from Hericium erinaceus on the MODE-K/DCs co-culture model. *Int. J. Biol. Macromol.* **2021**, *187*, 272–280. [CrossRef] [PubMed]
38. Ren, Y.; Sun, Q.; Gao, R.; Sheng, Y.; Guan, T.; Li, W.; Zhou, L.; Liu, C.; Li, H.; Lu, Z.; et al. Low Weight Polysaccharide of Hericium erinaceus Ameliorates Colitis via Inhibiting the NLRP3 Inflammasome Activation in Association with Gut Microbiota Modulation. *Nutrients* **2023**, *15*, 739. [CrossRef] [PubMed]
39. Shao, S.; Wang, D.; Zheng, W.; Li, X.; Zhang, H.; Zhao, D.; Wang, M. A unique polysaccharide from Hericium erinaceus mycelium ameliorates acetic acid-induced ulcerative colitis rats by modulating the composition of the gut microbiota, short chain fatty acids levels and GPR41/43 respectors. *Int. Immunopharmacol.* **2019**, *71*, 411–422. [CrossRef] [PubMed]
40. Jimoh, O.A.; Daramola, O.T.; Okin-Aminu, H.O.; Ojo, O.A. Performance, hemato-biochemical indices and oxidative stress markers of broiler chicken fed phytogenic during heat stress condition. *J. Anim. Sci. Technol.* **2022**, *64*, 970–984. [CrossRef] [PubMed]
41. Liu, W.C.; Zhuang, D.; Zhao, Y.; Balasubramanian, B.; Zhao, Z. Seaweed-Derived Polysaccharides Attenuate Heat Stress-Induced Splenic Oxidative Stress and Inflammatory Response via Regulating Nrf2 and NF-κB Signaling Pathways. *Mar. Drugs* **2022**, *20*, 358. [CrossRef] [PubMed]
42. Lin, C.; Su, Z.; Luo, J.; Jiang, L.; Shen, S.C.; Zheng, W.; Gu, W.; Cao, Y.; Chen, Y. Polysaccharide extracted from the leaves of Cyclocarya paliurus (Batal.) Iljinskaja enhanced stress resistance in Caenorhabditis elegans via skn-1 and hsf-1. *Int. J. Biol. Macromol.* **2019**, *143*, 243–254. [CrossRef] [PubMed]
43. Tu, J.; Liu, H.; Wen, Y.; Chen, P.; Liu, Z. A novel polysaccharide from Hericium erinaceus: Preparation, structural characteristics, thermal stabilities, and antioxidant activities in vitro. *J. Food Biochem* **2021**, *45*, e13871. [CrossRef] [PubMed]
44. Qiu, F.; Luo, Y.; Chen, X.; Ren, Z.; Qin, T. Alleviation of heat stress-induced jejunal injury in ducks by Hericium erinaceus polysaccharide. *Poult. Sci.* **2025**, *105*, 106342. [CrossRef] [PubMed]

45. Hou, X.; Liu, J.; Li, Z.; Chang, M.; Guo, M.; Feng, C.; Shi, J. Fruiting body polysaccharides of Hericium erinaceus induce apoptosis in human colorectal cancer cells via ROS generation mediating caspase-9-dependent signaling pathways. *Food Funct.* **2020**, *11*, 6128–6138. [CrossRef] [PubMed]
46. Chen, N.; Jiang, T.; Xu, J.; Xi, W.; Shang, E.; Xiao, P.; Duan, J.A. The relationship between polysaccharide structure and its antioxidant activity needs to be systematically elucidated. *Int. J. Biol. Macromol.* **2024**, *270*, 132391. [CrossRef] [PubMed]
47. Zhu, J.; Thompson, C.B. Metabolic regulation of cell growth and proliferation. *Nat. Rev. Mol. Cell Biol.* **2019**, *20*, 436–450. [CrossRef] [PubMed]
48. Wani, S.M.; Gani, A.; Mir, S.A.; Masoodi, F.A.; Khanday, F.A. B-Glucan: A dual regulator of apoptosis and cell proliferation. *Int. J. Biol. Macromol.* **2021**, *182*, 1229–1237. [CrossRef] [PubMed]
49. Kang, S.; Yoo, J.; Myung, K. PCNA cycling dynamics during DNA replication and repair in mammals. *Trends Genet* **2024**, *40*, 526–539. [CrossRef] [PubMed]
50. Gan, Q.; Ding, Y.; Peng, M.; Chen, L.; Dong, J.; Hu, J.; Ma, Y. The Potential of Edible and Medicinal Resource Polysaccharides for Prevention and Treatment of Neurodegenerative Diseases. *Biomolecules* **2023**, *13*, 873. [CrossRef] [PubMed]
51. Zhou, W.; Zhao, Y.; Yan, Y.; Mi, J.; Lu, L.; Luo, Q.; Kellis, M.; Zeng, X.; Cao, Y. Antioxidant and immunomodulatory activities in vitro of polysaccharides from bee collected pollen of Chinese wolfberry. *Int. J. Biol. Macromol.* **2020**, *163*, 190–199. [CrossRef] [PubMed]
52. Liu, Y.; Yang, L.; Wang, J.; Song, L. Physicochemical and colon cancer HT-29 cell inhibitory property of homogeneous polysaccharide from Stropharia rugosoannulata. *Int. J. Biol. Macromol.* **2025**, *307*, 141975. [CrossRef] [PubMed]
53. Koszla, O.; Kukula-Koch, W.; Józwiak, K.; Jastraz, R.; Marc, M.A.; Mytych, J.; Tabecka-Lonczynska, A.; Skóra, B.; Szychowski, K.A.; Solek, P. Biotransformation of Ganoderma lucidum and Hericium erinaceus for ex vivo gut-brain axis modulation and mood-related outcomes in humans: CREB/BDNF signaling and microbiota-driven synergies. *J. Ethnopharmacol.* **2025**, *342*, 119393. [CrossRef] [PubMed]
54. Deretic, V.; Saitoh, T.; Akira, S. Autophagy in infection, inflammation and immunity. *Nat. Rev. Immunol.* **2013**, *13*, 722–737. [CrossRef] [PubMed]
55. Wang, S.H.; Cheng, C.Y.; Chen, C.J.; Chan, H.L.; Chen, H.H.; Tang, P.C.; Chen, C.F.; Lee, Y.P.; Huang, S.Y. Acute Heat Stress Changes Protein Expression in the Testes of a Broiler-Type Strain of Taiwan Country Chickens. *Anim. Biotechnol.* **2019**, *30*, 129–145. [CrossRef] [PubMed]
56. Ariyoshi, W.; Koga, A.; Kodama, Y.; Yamasaki, R.; Yoshioka, Y.N.; Usui, M.; Mochizuki, S.; Adachi, Y. Inhibition of osteoclast differentiation by (1→3)-β-D-glucan from Alcaligenes faecalis (curdlan) and dectin-1 interaction via the syk proteolytic system. *Carbohydr. Polym. Technol. Appl.* **2025**, *9*, 100683. [CrossRef]
57. Wang, X.; Zhang, D.; Yin, J.; Nie, S.; Xie, J. Recent developments in Hericium erinaceus polysaccharides: Extraction, purification, structural characteristics and biological activities. *Crit. Rev. Food Sci. Nutr.* **2018**, *59*, S96–S115. [CrossRef] [PubMed]
58. Xiao, H.; Wei, C.; Liu, H.; Li, Z.; Zheng, C.; Luo, J. Lentinan alleviates sciatic nerve injury by promoting autophagy to remove myelin fragments. *Phyther. Res.* **2023**, *37*, 4042–4058. [CrossRef] [PubMed]
59. Lin, Y.J.; Huang, C.Y.; Tsai, B.C.K.; Kumar, K.A.; Hsieh, D.J.Y.; Chiu, P.L.; Chang, Y.M.; Ho, T.J.; Kuo, W.W.; Ju, D.T. Alcoholic Hericium erinaceus mycelia extract induces SIRT-1/ERK-1/2 mediated autophagy to prevent accumulation and spreading of alpha-synuclein and amyloid-beta peptide on the A53T transgenic mice. *J. Funct. Foods* **2023**, *110*, 105874. [CrossRef]

Disclaimer/Publisher's Note: The statements, opinions and data contained in all publications are solely those of the individual author(s) and contributor(s) and not of MDPI and/or the editor(s). MDPI and/or the editor(s) disclaim responsibility for any injury to people or property resulting from any ideas, methods, instructions or products referred to in the content.